

# Controlling for population structure in bacterial association studies

Sarah G Earle<sup>1\*</sup>, Chieh-Hsi Wu<sup>1\*</sup>, Jane Charlesworth<sup>1\*</sup>, Nicole Stoesser<sup>1</sup>, N Claire Gordon<sup>1</sup>, Timothy M Walker<sup>1</sup>, David A Clifton<sup>2</sup>, E Grace Smith<sup>3</sup>, Nazir Ismail<sup>4</sup>, Martin J Llewelyn<sup>5</sup>, Tim E Peto<sup>1</sup>, Derrick W Crook<sup>1</sup>, Gil McVean<sup>6</sup>, A Sarah Walker<sup>1</sup>, Daniel J Wilson<sup>1,6</sup>

Addresses:

<sup>1</sup> Nuffield Department of Medicine, University of Oxford, John Radcliffe Hospital, Oxford, OX3 9DU, United Kingdom

<sup>2</sup> Institute of Biomedical Engineering, Department of Engineering Science, University of Oxford, Oxford, United Kingdom

<sup>3</sup> Public Health England, West Midlands Public Health Laboratory, Heartlands Hospital, Birmingham, United Kingdom

<sup>4</sup> Centre for Tuberculosis, National Institute for Communicable Diseases, Johannesburg, South Africa

<sup>5</sup> Department of Infectious Diseases and Microbiology, Royal Sussex County Hospital, Brighton, United Kingdom

<sup>6</sup> Wellcome Trust Centre for Human Genetics, University of Oxford, Roosevelt Drive, Oxford, OX3 7BN, United Kingdom

\* These authors contributed equally

Corresponding author D.J.W. Email: [daniel.wilson@ndm.ox.ac.uk](mailto:daniel.wilson@ndm.ox.ac.uk)

## Abstract

Bacteria pose unique challenges for genome-wide association studies (GWAS) because of strong structuring into distinct strains and substantial linkage disequilibrium across the genome. While methods developed for human studies can correct for strain structure, this risks considerable loss-of-power because genetic differences between strains often contribute substantial phenotypic variability. Here we propose a new method that captures lineage-level associations even when locus-specific associations cannot be fine-mapped. We demonstrate its ability to detect genes and genetic variants underlying resistance to 17 antimicrobials in 3363 isolates from four taxonomically diverse clonal and recombining bacteria: *Mycobacterium tuberculosis*, *Staphylococcus aureus*, *Escherichia coli* and *Klebsiella pneumoniae*. Strong selection, recombination and penetrance confer high power to recover known antimicrobial resistance mechanisms, and reveal a novel association between the outer membrane porin *nmpC* and cefazolin resistance in *E. coli*. Hence our method pinpoints locus-specific effects where possible, and boosts power by detecting lineage-level differences when fine-mapping is intractable.

## Intro

Mapping genetic variants underlying bacterial phenotypic variability is of great interest owing to the metabolic diversity and fundamental role of bacteria ecologically, economically and in the global burden of disease<sup>1-6</sup>. Hospital-associated infections including *Staphylococcus aureus*, *Escherichia coli* and *Klebsiella pneumoniae* represent a serious threat to the safe provision of healthcare<sup>7-9</sup>, while the *Mycobacterium tuberculosis* pandemic remains a major global health challenge. Treatment options continue to be eroded by the spread of antimicrobial resistance, with some strains resistant even to antimicrobials of last resort<sup>10</sup>.

GWAS offers new opportunities to map bacterial phenotypes<sup>11-24</sup>, presenting certain advantages in bacteria including inexpensive sequencing of entire genomes enabling direct analysis of causal loci and functional validation via well-developed molecular approaches. However, bacterial populations typically exhibit genome-wide LD and strong structuring into geographically-widespread genetic

lineages or strains that are likely maintained by selection<sup>25,26</sup>. Approaches to controlling for this population structure have allowed for systematic phenotypic differences based on cluster membership<sup>19,20</sup> or, in clonal species, phylogenetic history<sup>17,23,24</sup>. However, these and other approaches common in human GWAS<sup>27-29</sup> risk low power because differences between strains account for large proportions of both phenotypic and genetic variability.

Here we describe a new approach for controlling bacterial population structure based on linear mixed models (LMMs). LMMs capture the fine structure of populations more faithfully than clustering approaches, and enjoy greater applicability than phylogenetic approaches since recombination is evident in most bacteria<sup>30,31</sup>. We adapt the LMM approach to boost power by recovering signals of lineage-level associations when associations cannot be pinpointed to individual loci, without sacrificing power to detect locus-specific associations.

## Results

### Controlling for population structure risks widespread loss of power in bacteria

Controlling for population structure aims to avoid spurious associations arising from (i) LD with genuine causal variants that are population-stratified, (ii) uncontrolled environmental variables that are population-stratified, and (iii) population-stratified differences in sampling<sup>28,29</sup>. In the species we investigated, we observed genome-wide LD and strong population structure, with the first 10 principal components (PCs<sup>32</sup>) explaining 70-93% of genetic variation, compared to 27% in human chromosome 1 (**Supplementary Figs. 1, 2**). Controlling artefacts arising from population structure therefore risks loss of power to detect genuine associations in this large proportion of population-stratified loci.

Empirically, we observed loss in significance at the population-stratified *far* locus in *S. aureus*, a mobile-element-associated gene encoding resistance to the antimicrobial fusidic acid<sup>33-36</sup>. The Far protein prevents fusidic acid interacting with its target EF-G. We tested for associations between fusidic acid resistance and the presence or absence of short 31bp haplotypes or *kmers*<sup>17</sup> (**Supplementary Fig. 3a**). This approach aims to capture resistance encoded by substitutions in the core genome, the presence of mobile accessory genes, or both.

Kmers linked to the presence of *far* showed the strongest genome-wide association with fusidic acid resistance ( $p < 10^{-122}$ ) by  $\chi^2$  test. However, *far*-encoded resistance was associated exclusively with strains ST-1 and 8. Controlling for population structure using LMM<sup>37,38</sup> reduced significance to  $p < 10^{-39}$  (**Fig. 1a**), below other loci including *fusA*, which encodes EF-G. Kmers capturing unstratified low-frequency resistance-conferring substitutions in *fusA* were propelled to greater significance ( $p < 10^{-11}$  by  $\chi^2$  test,  $p < 10^{-157}$  by LMM) because LMM can increase power in the presence of polygenic effects<sup>39</sup>. However, *fusA* variants explain a smaller proportion of resistance overall than *far*.

While kmers linked to *far* did not suffer outright loss of significance because penetrance is high for antibiotic resistance, simulations show that for phenotypes with modest effect sizes (e.g. odds ratios of 3), controlling for population structure risks loss of genome-wide significance at 59%, 75%, 99% and 99% of high-frequency causal variants in *M. tuberculosis* ( $n = 1954$ ), *S. aureus* ( $n = 992$ ), *E. coli* ( $n = 241$ ) and *K. pneumoniae* ( $n = 176$ ) respectively, with power loss greatest when sample size is low and the number of variants is high (**Fig. 2a, Supplementary Fig. 4a**).

### Detecting lineage- versus locus-specific associations

Limiting loss of power using leave-one-chromosome-out<sup>39,40</sup> is impractical in bacteria, which typically have one chromosome. Instead we developed a method to recover information discarded when controlling for population structure. In cases where population stratification reduces power to detect locus-specific associations, our method infers lineage-specific associations, similar to a

phylogenetic regression<sup>41,42</sup>, without sacrificing power to detect locus-specific associations when able to do so.

We observed that leading PCs tend to correspond to major lineages in bacterial genealogies (or *clonal frames*<sup>43-45</sup>) (**Fig. 1b**), reflecting an underlying relationship between genealogical history and PC analysis<sup>46</sup>. The use of PCs to control for population structure allows coefficients to be estimated that capture lineage-level phenotypic differences. LMMs are connected to PC analysis because the random effects that allow every locus to exert a small, but cumulatively potentially large, phenotypic effect can be reinterpreted as allowing every PC to exert a phenotypic effect<sup>47</sup>. Therefore we decomposed the random effects from the LMM to obtain an estimated coefficient and standard error for each PC (see Methods). We then employed a Wald test<sup>48</sup> to assess the significance of the association between each lineage and the phenotype. By defining lineages as PCs, we minimize loss-of-power caused by correlations between lineages.

Our method, implemented in the R package *bugwas*, revealed strong signals of association between fusidic acid resistance and lineages including PCs 6 and 9 ( $p < 10^{-70}$ ) (**Fig. 1c, Supplementary Fig. 5**), comparable in significance to the low-frequency variants at *farA*. We then reassessed locus-specific effects by assigning variants to lineages according to the PC to which they were most correlated, and comparing the significance of variants within lineages. This showed that *far* and variants in LD with *far* accounted for the strongest signals within PCs 6 and 9 ( $p < 10^{-34}$  and  $10^{-45}$  respectively) (**Fig. 1d**). In simulations, our method was able to recover signals of lineage-level associations in cases where significance at individual loci was lost by controlling for population structure, increasing power 2.5- (*M. tuberculosis*) to 22.0-fold (*E. coli*) (**Fig. 2a, Supplementary Fig. 4a**).

The strongest locus-specific associations of lineages PC 6 and 9 localized to a 20kb region containing the staphylococcal cassette chromosome (SCC), the most significant hit mapping to the gene adjacent to *far*. However, simulations showed that fine-mapping will frequently suffer from genome-wide LD because LD is not generally organized into physically linked blocks along the chromosome (**Fig. 2b, Supplementary Fig. 4b**).

### **The ability of bacterial GWAS to identify antimicrobial resistance determinants**

Confronted with strong population structure and genome-wide LD in bacteria, we wished to test empirically the ability of GWAS to pinpoint genuine causal variants more generally. Therefore we conducted 26 GWAS for resistance to 17 antimicrobials in 3363 isolates across the major pathogens *M. tuberculosis*<sup>49</sup>, *S. aureus*<sup>50</sup>, *E. coli* and *K. pneumoniae*<sup>51</sup> (**Supplementary Fig. 6**).

We supplemented the kmer approach by surveying variation in SNPs and gene presence or absence. We imputed missing SNP calls by reconstructing the clonal frame<sup>43,45</sup> followed by ancestral state reconstruction<sup>52</sup>, an approach that generally outperformed imputation using Beagle<sup>53</sup> (**Supplementary Table 2**).

### **Multi-drug resistance and multisite resistance mechanisms compromise signals of association**

Correlated phenotypes caused by the presence of multi-drug resistant isolates led to significant results in unexpected loci or regions in some analyses. A combination of first-line drug regimens contributes to multi-drug resistance co-occurrence in *M. tuberculosis*, which led to spurious associations as the top hit before controlling for population structure between ethambutol and pyrazinamide resistance and SNPs in rifampicin resistance-conferring *rpoB*. Even after controlling for population structure, these associations remained genome-wide significant at  $p < 10^{-45}$  and  $p < 10^{-54}$ .

Antimicrobial resistance has arisen over 20 times per drug in the *M. tuberculosis* tree, through frequent convergent evolution (**Supplementary Fig. 6, Supplementary Fig. 4c**). Within a single gene, such as *rpoB*, there are multiple targets for selection. Both SNP and kmer-based approaches correctly identified variants in known resistance-causing codons, but greater significance was attained in the latter since the targets for selection were typically within 31bp (**Supplementary Fig. 7**). In these cases, absence of the wild type allele was found to confer resistance, with power gained by pooling over the alternative mutant alleles.

### **Strong selection and recombination assist fine-mapping of antibiotic resistance determinants**

For each drug and species, we evaluated whether GWAS identified a genuine causal variant as the most significant hit. By this measure, the performance of GWAS across species was very good, identifying genuine causal loci or regions in physical linkage with those loci for antimicrobial resistance in 25/26 cases for the SNP and gene approach and the kmer approach after controlling for population structure (**Table 1**). Particularly for accessory genes such as  $\beta$ -lactamases, mobile element-associated regions of LD were often detected along with the causal locus (**Supplementary Data 1**).

Genuine resistance-conferring variants were detected in all but one study, demonstrating that the high accuracy attained in predicting antimicrobial resistance phenotype from genotypes known from the literature<sup>50,54</sup> is mirrored by good power to map the genotypes that confer antimicrobial resistance phenotypes using GWAS. However, these results also reflect extraordinary selection pressures exerted by antimicrobials. High homoplasy at resistance-conferring loci caused by repeat mutation and recombination break down LD, assisting mapping (**Fig. 2c, Supplementary Fig. 4c**).

For one drug, cefazolin, in *E. coli*, we identified variation in the presence of an unexpected gene as the most strongly associated with resistance, *nmpC* ( $p = 10^{-12.4}$ ). NmpC is an outer membrane porin over-represented in susceptible individuals. Permeability in the *Salmonella typhimurium* homolog mediates resistance to other cephalosporin beta-lactams, making this a strong candidate for a novel resistance-conferring mechanism discovered in *E. coli*.

### **Conclusion**

Population structure presents the greatest challenge for GWAS in bacteria, because of the inherent trade-off between power to detect genuine associations of population-stratified variants and robustness to unmeasured, population-stratified confounders. By introducing a test for lineage-specific associations, we allow these signals to be recovered even in the absence of homoplasy, while acknowledging the increased risk of confounding. Identifying the most significant lineage-associated loci provides greater flexibility in the interpretation of bacterial GWAS by permitting the pursuit of functional validation within potentially large groups of lineage-associated variants that collectively show a strong signal of phenotypic association, but which cannot be distinguished statistically. While such a strategy affords improved power to detect population-stratified variants of large effect, it carries risks, because lineage-associated effects are more susceptible to confounding with population-stratified differences in environment or sampling. This trade-off between power and robustness underlines the importance of functional validation for bacterial GWAS.

### **Methods**

**Linear mixed model.** In the linear mixed model<sup>37-40</sup> (LMM), the phenotype is modelled as  
 $phenotype = covariates + foreground\ locus + background\ loci + environment$

Formally,

$$y_i = W_{i1}\alpha_1 + \dots + W_{ic}\alpha_c + X_{il}\beta_l + X_{i1}\gamma_1 + \dots + X_{iL}\gamma_L + \varepsilon_i,$$

where there are  $n$  individuals,  $c$  covariates including an intercept,  $L$  loci,  $l$  is the foreground locus,  $y_i$  is the phenotype in individual  $i$ ,  $W_{ij}$  is covariate  $j$  in individual  $i$ ,  $\alpha_j$  is the effect of covariate  $j$ ,  $X_{ij}$  is the genotype of locus  $j$  in individual  $i$ ,  $\beta_l$  is the foreground effect of locus  $l$ ,  $\gamma_j$  is the background effect of locus  $j$  and  $\varepsilon_i$  is the effect of the environment (or error) on individual  $i$ . Biallelic genotypes are encoded as  $-f_j$  (common allele) or  $1-f_j$  (rare allele), where  $f_j$  is the frequency of the rare allele at locus  $j$ . This ensures that the mean value of  $X_{ij}$  over individuals  $i$  is zero for any locus  $j$ . Since triallelic and tetraallelic loci are rare, we use only biallelic loci to model background effects. When the foreground locus is triallelic ( $K = 3$ ) or tetraallelic ( $K = 4$ ), the genotype in individual  $i$  is encoded as a vector indicating the presence (1) or absence (0) of the first ( $K-1$ ) alleles and  $\beta_l$  becomes a vector of length ( $K-1$ ).

The background effects of the loci are treated as random effects, meaning the precise values of the coefficients  $\gamma_j$  are averaged over. The  $\gamma_j$ s are assumed to follow independent normal distributions with common mean 0 and variance  $\lambda\tau^{-1}$ . Since most loci are expected to have little or no effect on a particular phenotype, this tends to constrain the magnitude of the background effect sizes to be small. The environmental effects are also treated as random effects assumed to follow independent normal distributions with mean 0 and variance  $\tau^{-1}$ . The model can be rewritten in matrix form as

$$\mathbf{y} = \mathbf{W} \boldsymbol{\alpha} + \mathbf{X}_{\cdot l} \beta_l + \mathbf{u} + \boldsymbol{\varepsilon}$$

with

$$\begin{aligned} \mathbf{u} &= \mathbf{X}_{\cdot 1} \gamma_1 + \dots + \mathbf{X}_{\cdot L} \gamma_L \\ \mathbf{u} &\sim \text{MVN}_n(0, \lambda \tau^{-1} \mathbf{K}) \\ \boldsymbol{\varepsilon} &\sim \text{MVN}_n(0, \tau^{-1} \mathbf{I}_n) \end{aligned}$$

where  $\mathbf{u}$  represents the cumulative background effects of the loci, MVN denotes the multivariate normal distribution,  $\mathbf{I}_n$  is an  $n \times n$  identity matrix and  $\mathbf{K}$  is an  $n \times n$  relatedness matrix defined as  $\mathbf{K} = \mathbf{X} \mathbf{X}'$ .

**Testing for locus effects.** To assess the significance of the effect of an individual locus  $l$  on the phenotype, controlling for population structure and background genetic effects, the parameters of the linear mixed model  $\alpha_1 \dots \alpha_c$ ,  $\beta_l$ ,  $\lambda$  and  $\tau$  were estimated by maximum likelihood and a likelihood ratio test with  $(K-1)$  degrees of freedom was performed against the null hypothesis that  $\beta_l = 0$  using the software GEMMA<sup>38</sup>.

**Testing for lineage effects.** Since controlling for population structure drastically reduces power at population-stratified variants, and since a large proportion of variants are typically population-stratified in bacteria, we recovered information from the LMM regarding lineage-level differences in phenotype.

We defined lineages using principal components (PCs) because we observed that PCs tend to trace paths through the clonal frame genealogy corresponding to recognizable lineages and because PCs are mutually uncorrelated, minimizing loss-of-power to detect differences between lineages due to correlations. PCs were computed based on biallelic SNPs using the R function `prcomp()`, producing an  $L$  by  $n$  loading matrix  $\mathbf{W}$  and an  $n$  by  $n$  score matrix  $\mathbf{T}$  where  $\mathbf{T} = \mathbf{X}\mathbf{W}$ .  $W_{ij}$  records the contribution of biallelic SNP  $i$  to the definition of PC  $j$  while  $T_{ij}$  represents the projection of individual  $i$  on to PC  $j$ .

Point estimates and standard errors for the background locus effects are usually overlooked because the assumed normal distribution with common mean 0 and variance  $\lambda\tau^{-1}$  tends to cause them to be small in magnitude and not significantly different from zero. However, cumulatively the background locus effects can capture systematic phenotypic differences between lineages. Therefore we recovered the post-data distribution (analogous to a posterior distribution) of the background locus random effects,  $\boldsymbol{\gamma}$ , from the LMM.

Empirically, we found that the post-data distribution of the background random effects was generally insensitive to the identity of the foreground locus and comparable under the null hypothesis ( $\beta_l = 0$ ). Therefore, we calculated the mean and variance-covariance matrix of the multivariate normal post-data distribution of  $\boldsymbol{\gamma}$  in the LMM null model. These are equivalent to those of a ridge regression<sup>55</sup>, and were computed as

$$\boldsymbol{\mu} = (\mathbf{X}'\mathbf{X} + 1/\lambda \mathbf{I}_L)^{-1} \mathbf{X}'\mathbf{y} \text{ and } \boldsymbol{\Sigma} = (\tau \mathbf{X}'\mathbf{X} + 1/\lambda \mathbf{I}_L)^{-1}$$

respectively. Both  $\lambda$  and  $\tau$  were estimated by GEMMA under the LMM null model.

Using the inverse transformation of the biallelic variants from PCA,  $\mathbf{X} = \mathbf{T} \mathbf{W}^{-1}$ , the background random effects can be rewritten in terms of the contribution of the  $n$  PCs

$$\begin{aligned} \mathbf{u} &= \mathbf{X}_{\cdot 1} \gamma_1 + \dots + \mathbf{X}_{\cdot L} \gamma_L \\ &= \mathbf{X} \boldsymbol{\gamma} = \mathbf{T} \mathbf{W}^{-1} \boldsymbol{\gamma} = \mathbf{T} \mathbf{g} \\ &= \mathbf{T}_{\cdot 1} g_1 + \dots + \mathbf{T}_{\cdot n} g_n \end{aligned}$$

where  $\mathbf{g} = \mathbf{W}^{-1} \boldsymbol{\gamma}$ ,  $g_j$  being the background effect of PC  $j$  on the phenotype. We therefore computed the mean and variance of the post-data distribution of  $\mathbf{g}$  as  $\mathbf{m} = \mathbf{W}^{-1} \boldsymbol{\mu}$  and  $\mathbf{S} = \mathbf{W}^{-1} \boldsymbol{\Sigma} \mathbf{W}$  respectively using the affine transformation for a multivariate normal distribution. To test the null hypothesis of no background effect of PC  $j$  (i.e.  $g_j = 0$ ) we employed a Wald test with test statistic  $w_j = m_j^2/S_{jj}$ , which we compared against a chi-squared distribution with one degree of freedom to obtain a  $p$ -value.

**Identifying non genome-wide PCs.** Some PCs capture variation localized to particular areas of the genome. We identified non genome-wide PCs by testing for spatial heterogeneity of the loading matrix  $\mathbf{W}$  for biallelic SNPs across the genome. SNPs were grouped into 20 contiguous bins (indexed by  $j$ ) of nearly equal sizes  $N_j$  and the mean  $O_{ij}$  and variance  $V_{ij}$  in the absolute value of the SNP loadings for PC  $i$  in bin  $j$  were calculated, along with the mean absolute value  $E_i$  of the SNP loadings for PC  $i$  across all SNPs. The null hypothesis of no heterogeneity was assessed by comparing the test statistic  $\chi_i^2 = \sum_j (O_{ij} - E_i)^2 / (V_{ij}/N_j)$  to a chi-squared distribution with degrees of freedom equal to the number of bins minus one to obtain a  $p$ -value.

**Whole genome sequencing and SNP calling.** DNA was extracted and sequenced using the Illumina HiSeq 2000 platform (San Diego, CA, USA) as described previously<sup>56,57</sup>. Reads were mapped using Stampy<sup>58</sup> to reference strains CFT073 (genbank accession AE014075.1), MGH 78578 (CP000647.1), H37Rv (NC\_000962.2) and MRSA252 (BX571856.1) for *Escherichia coli*, *Klebsiella pneumoniae*, *Mycobacterium tuberculosis* and *Staphylococcus aureus* respectively.

**Defining the pan-genome.** In order to investigate gene presence or absence we created a pan-genome for each set of isolates. To obtain whole genome assemblies, reads were *de novo* assembled using Velvet<sup>59</sup>. We annotated open reading frames on the *de novo* assemblies for each isolate. We then used the Bayesian gene-finding program Prodigal<sup>60</sup> to identify a set of protein sequences for each *de novo* assembly. These annotated protein sequences were clustered using CD-hit<sup>61</sup> with a clustering threshold of 70% identity across 70% of the longer sequence. We converted the output of CD-hit into a matrix of binary genotypes denoting presence or absence of each gene cluster in each genome (**Supplementary Fig. 3b**).

**Kmer counting.** Some diversity such as indels and repeats is difficult to capture using standard variant calling tools. To capture non-SNP variation, we pursued a kmer or word-based approach<sup>17</sup> in which all unique 31 base haplotypes were counted from the sequencing reads using dsk<sup>62</sup> following adaptor trimming and removal of duplicates and low quality reads using Trimmomatic<sup>63</sup>. If a kmer was counted five or more times in an isolate, then it was counted as present, and if not it was treated as absent. This produced a deduplicated set of variably present kmers across the dataset, with the presence or absence of each determined per isolate. The total number of SNPs, kmers and gene clusters per species can be found in **Supplementary Table 1**.

**Phylogenetic inference.** Maximum likelihood phylogenies were estimated for visualization and SNP imputation purposes using RAxML version 7.7.6<sup>64</sup>, with a GTR model and no rate heterogeneity, using alignments from the mapped data based on biallelic sites, with non-biallelic sites being set to the reference, using the command line "raxmlHPC-PTHREADS-SSE3 -s phylipFile -n outputPrefix -m GTRCAT -p 12345 -c 1 -T 2 -D ON -f c -F ON -V".

**SNP imputation.** Since Illumina sequencing is inherently more error-prone than Sanger sequencing, strict filtering is required for reliable mapping-based SNP calling, contributing to a small but appreciable frequency of uncalled bases in the genome due to ambiguity or deletion. Restricting analysis to sites called in all genomes is undesirable, while ignoring uncalled sites by removing individuals with missing data at individual sites generates  $p$ -values that cannot be validly compared between sites because they are calculated using data from differing sets of isolates. Instead we imputed the missing base calls using two approaches, ClonalFrameML<sup>45</sup> and Beagle<sup>53</sup>.

Imputation using ClonalFrameML<sup>45</sup> involves jointly reconstructing ancestral states and missing base calls by maximum likelihood utilizing the phylogeny reconstructed earlier<sup>65</sup>. ClonalFrameML was run using the command line "cat fastaFile.fa | ./ClonalFrameML phylogenyFile /dev/stdin 1 outputPrefix --correct\_branch\_length false". To use Beagle the mapped data was coded as haploid (one column per individual), and input as phased data<sup>53,66</sup>. Beagle was run using the command line "java -Djava.io.tmpdir=/tempDir -Xmx150000m -jar beagle-2.jar phased=beagleData missing=N out=outputPrefix".

**Testing imputation accuracy.** To simulate data for testing imputation accuracy, 100 sequences were randomly sampled from each GWAS dataset across the phylogeny. Maximum likelihood phylogenies were estimated for the 100 sequences of each species using RAxML<sup>64</sup> as above. Any columns in the alignment corresponding to ambiguous bases in the reference genome were excluded. One round of imputation was performed using ClonalFrameML to produce complete datasets with no ambiguous bases (Ns) that were then treated as the truth for the purpose of testing. The empirical distributions of Ns per site in the datasets of 100 sequences were determined, and these were sampled with replacement to reintroduce Ns to the variable sites in 100 simulated datasets. These sequences were then imputed again using ClonalFrameML and Beagle. Accuracy was summarized per site as a function of the frequency of Ns per site and the minor allele frequency. Overall ClonalFrameML was more accurate than Beagle, thus ClonalFrameML was used for all GWAS analyses (**Supplementary Table 1**).

**Calculating association statistics before controlling population structure.** We wished to compare the significance of associations before and after controlling for population structure. For the SNP and gene presence or absence data, an association between each SNP or gene and the phenotype was tested by logistic regression implemented in R. For the kmer analyses, an association between the presence or absence of each kmer was tested using a  $\chi^2$  test implemented in C++. For each variant a  $p$ -value was computed.

**Correction for multiple testing.** Multiple testing was accounted for by applying a Bonferroni correction<sup>67</sup>; the individual locus effect of a variant (SNP, gene or kmer) was considered significant if its  $p$ -value was smaller than  $\alpha/n_p$  where we took  $\alpha = 0.05$  to be the genome-wide false positive rate and  $n_p$  to be the number of SNPs and genes with unique phylogenetic patterns, i.e. unique partitions of individuals according to allele membership. Since the phenotypic contribution of multiple variants with identical phylogenetic patterns cannot be disentangled statistically, we found that pooling such variants improved power by demanding a less conservative Bonferroni correction than correcting for the total number of variants.

We employed the same thresholds for assessing kmer significance because the number of variants in the population is not fundamentally different, but multiple kmers tag any given variant. The genome-wide  $-\log_{10} p$ -value threshold was 5.3 for *S. aureus* ciprofloxacin, erythromycin, fusidic acid, gentamicin, penicillin, methicillin, tetracycline and rifampicin, 5.2 for *S. aureus* trimethoprim, 5.8 for all antimicrobials tested for *E. coli*, 5.9 for all antimicrobials tested for *K. pneumoniae*, and 4.3 for all antimicrobials tested for *M. tuberculosis*. We also accounted for multiple testing of lineage effects by applying a Bonferroni correction for the number of PCs, which equals the sample size  $n$ .

**Running GEMMA.** For the analyses of SNPs, genes and kmers, we computed the relatedness matrix  $\mathbf{K}$  from biallelic SNPs only. We tested for foreground effects at all biallelic, triallelic and tetrallelic SNPs, genes and kmers. GEMMA was run using a minor allele frequency of 0 to include all SNPs. To calculate  $\mathbf{K}$ , GEMMA was run using the command line on biallelic SNPs `./gemma -g genFile -a snpFile -p phenotypeFile -gk 1 -o outputPrefix -maf 0`. Foreground effects were tested using the command line `./gemma -g genFile -a snpFile -p phenotypeFile -k relatednessMatrix -c o-lmm 4 -o outputPrefix -maf 0`. GEMMA was modified to output the ML log-likelihood under the null and alternative, and  $-\log_{10} p$ -values were calculated using the following command in R: `log10(exp(1)) * pchisq((2 * (LA - L0)), numAlleles - 1, low = F, log=TRUE)`, where LA is the ML log-likelihood under the alternative for that variant, L0 is the ML log-likelihood under the null determined using biallelic SNPs and numAlleles is the number of alleles ( $K$ ) at that site.

To perform LMM on tri- and tetra-allelic SNPs, each SNP was encoded as  $K-1$  binary columns corresponding to the first  $K-1$  alleles. For each column, an individual was encoded 1 if it contained that allele and 0 otherwise. The first column was input as the genotype, and the others as covariates into GEMMA, which was run using the command line: `./gemma -g genFile -a snpFile -p phenotypeFile -k relatednessMatrix -c covariatesFile o-lmm 4 -o outputPrefix -maf 0`. The log likelihood of the null from the biallelic SNPs along with the log likelihood under the alternative for each of the SNPs were used to calculate the  $p$ -value per SNP, using the R command above.

Due to the large number of kmers present within each dataset, it was not feasible to run LMM on all kmers. Thus we applied the LMM to the top 200,000 most significant kmers from the logistic regression, plus 200,000 randomly selected kmers of those remaining. The randomly selected kmers were used to indicate whether some were becoming relatively more significant than the top 200,000, providing a warning in case large numbers of kmers became significant only after controlling for population structure.

**Variant annotation.** SNPs were annotated in R using the reference fasta and genbank files to determine SNP type (synonymous, non-synonymous, nonsense, read-through, intergenic), the codon and codon position, reference and non-reference amino acid, gene name and gene product.

Unlike the SNP approach where we can easily refer to the reference genome to find what gene the SNP is in and the effect that it may have, annotation of the kmers is more difficult. We used BLAST<sup>68</sup> to identify the kmers in databases of annotated sequences. Each kmer was first annotated against a BLAST database created of all refseq genomes of the relevant genus on NCBI. This enabled automatic annotation of all kmers that gave a sufficiently small  $e$ -value against the genus specific database. All kmers were also searched against the whole nucleotide NCBI database, firstly to compare and confirm the matches made against the first database, and secondly to annotate the kmers that did not match to anything in the within-genus database. Finally, when the resistance determining mechanism was a SNP, the top 10000 kmers were mapped to a relevant reference genome using Bowtie2<sup>69</sup> using the command line `bowtie2 -r -D 24 -R 3 -N 0 -L 18 -i S,1,0.30 -x bowtieRef -U kmersToMap -S outputFile`. This was used to determine whether the most



significant kmers covered the position of the resistance causing SNP or whether they were found elsewhere in the gene.

Genes were annotated for each CD-hit gene cluster by performing BLAST<sup>68</sup> searches of each cluster sequence against a database of curated protein sequences downloaded from UNIPROT<sup>70</sup>.

**Testing power by simulating phenotypes.** To assess the performance of the method for controlling population structure, we performed 100 simulations per species. In each simulation, a biallelic SNP was randomly chosen among those SNPs with minor allele frequency above 20% to be the causal SNP. Binary phenotypes (case or control) were then simulated for each genome with case probabilities of 0.25 and 0.5 respectively in individuals with the common and rare allele at the causal SNP (an odds ratio of 3). For each simulated dataset, we tested for locus effects at every biallelic SNP and lineage effects at every PC, as described above. Power to detect locus effects was defined as the proportion of simulations in which the causal SNP was found to have a significant locus effect. This was compared to a theoretically optimum power computed as the proportion of simulations in which the causal SNP was found to have a significant locus effect when population structure and multiple testing were not controlled for. Power to detect lineage effects was computed as the proportion of simulations in which the PC most strongly correlated to the causal SNP was found to have a significant lineage effect. We defined fine mapping precision as the distance spanned by SNPs within two log-likelihoods of the most significant SNP in the test for locus effects, in those simulations in which the causal locus was genome-wide significant. We calculated the number of homoplasies per SNP by counting the number of branches in the phylogeny affected by a substitution based on the ClonalFrameML ancestral state reconstruction, and subtracting the minimum number of substitutions ( $K-1$ ).

**Software.** We have created an R package *bugwas* implementing our method for controlling population structure and an end-to-end GWAS pipeline using R, Python and C++. Both can be downloaded from [www.danielwilson.me.uk/virulogenomics.html](http://www.danielwilson.me.uk/virulogenomics.html).

## References

1. Whitman WB, Coleman DC, Wiebe WJ (1998) Prokaryotes: the unseen majority. *Proc Natl Acad Sci USA* 95: 6578-6583.
2. Hong SH, Bunge J, Jeon SO, Epstein SS (2006) Predicting microbial species richness. *Proc Natl Acad Sci USA* 103: 117-122.
3. Falkowski PG, Fenchel T, Delong EF (2008) The microbial engines that drive earth's biogeochemical cycles. *Science* 320: 1034-1039.
4. World Health Organization (2008) *The global burden of disease: 2004 update*. [http://www.who.int/healthinfo/global\\_burden\\_disease](http://www.who.int/healthinfo/global_burden_disease)
5. Didelot X, Bowden R, Wilson DJ, Peto TE, Crook DW (2012) Transforming clinical microbiology with bacterial genome sequencing. *Nat Rev Genet* 13: 601-612.
6. Wilson DJ (2012) Insights from genomics into bacterial pathogen populations. *PLoS Pathog* 8: e1002874.
7. Davies J, Davies D (2010) Origins and evolution of antibiotic resistance. *Microbiol Mol Biol Rev* 74: 417-433.
8. Nordmann P, Poirel L, Walsh TR, Livermore DM (2011) The emerging NDM carbapenemases. *Trends Microbiol* 19: 588-595.
9. European Centre for Disease Prevention and Control (2012) *Surveillance of surgical-site infections in Europe, 2008-2009*. [http://www.ecdc.europa.eu/en/publications/Publications/120215\\_SUR\\_SSI\\_2008-2009.pdf](http://www.ecdc.europa.eu/en/publications/Publications/120215_SUR_SSI_2008-2009.pdf)
10. World Health Organization (2014) *Antimicrobial Resistance: A Global Report on Surveillance*. World Health Organization, 20 Avenue Appia, 1211 Geneva 27, Switzerland.

11. Falush D, Bowden R (2006) Genome-wide association mapping in bacteria? *Trends Microbiol* 14: 353-355.
12. Bille E, et al. (2005) A chromosomally integrated bacteriophage in invasive meningococci. *J Exp Med* 201: 1905-1913.
13. Hotopp JCD, et al. (2006) Comparative genomics of *Neisseria meningitidis*: core genome, islands of horizontal transfer and pathogen-specific genes. *Microbiology* 152: 3733-3749.
14. Lindsay JA, et al. (2006) Microarrays reveal that each of the ten dominant lineages of *Staphylococcus aureus* has a unique combination of surface-associated and regulatory genes. *J Bacteriol* 188: 669-676.
15. Griswold A (2008) Genetic origins of microbial virulence. *Nat Educ* 1.
16. Peacock SJ, et al. (2002) Virulent combinations of adhesin and toxin genes in natural populations of *Staphylococcus aureus*. *Infect Immun* 70: 4987-4996.
17. Sheppard, S. K., Didelot, X., Meric, G., Torralbo, A., Jolley, K. A., Kelly, D. J., Bentley, S. D., Maiden, M. C. J., Parkhill, J. & Falush, D. (2013) Genome-wide association study identifies vitamin B5 biosynthesis as a host specificity factor in *Campylobacter*. *Proc Natl Acad Sci USA* 110, 11923-11927.
18. Alam, M. T., Petit III, R. A., Crispell, E. K., Thornton, T. A., Conneely, K. N., Jiang, Y., Satola, S. W., & Read, T. D. (2014). Dissecting vancomycin-intermediate resistance in *Staphylococcus aureus* using genome-wide association. *Genome Biol Evol* 6, 1174-1185.
19. Laabei, M., Recker, M., Rudkin, J. K., Aldejawi, M., Gulay, Z., Sloan, T. J., Williams, P., Endres, J.L, Bayles, K. W. & other authors (2014). *Genome Res* 24, 839-849.
20. Chewapreecha, C., Marttinen, P., Croucher, N. J., Salter, S. J., Harris, S. R., Mather, A. E., Hanage, W. P., Goldblatt, D., Nosten, F. H. & other authors (2014). Comprehensive identification of single nucleotide polymorphisms associated with beta-lactam resistance within pneumococcal mosaic genes. *PLoS Genet* 10, e1004547.
21. Salipante, S. J., Roach, D. J., Kitzman, J. O., Snyder, M. W., Stackhouse, B., Butler-Wu, S. M., Lee, C., Cookson, B. T. & Shendure, J. (2014). Large-scale genomic sequencing of extraintestinal pathogenic *Escherichia coli* strains. *Genome Res* 25, 119-128.
22. Read, T.D. & Massey, R. C. (2014). Characterizing the genetic basis of bacterial phenotypes using genome-wide association studies: a new direction for bacteriology. *Genome Med* 6, 109.
23. Fahrat, M. R., Shapiro, B. J., Sheppard, S. K., Colijn, C. & Murray, M. (2014) A phylogeny-based sampling strategy and power calculator informs genome-wide associations study design for microbial pathogens. *Genome Med* 6, 101.
24. Chen, P. E. & Shapiro, B. J. (2015). The advent of genome-wide association studies for bacteria. *Current Op Microbiol* 25, 17-24.
25. Feil EJ, Spratt BG (2001) Recombination and the structures of bacterial pathogens. *Annu Rev Microbiol* 55: 561-590.
26. Cordero, O. X., Polz, M. F. (2014) Explaining microbial genomic diversity in light of evolutionary ecology. *Nat Rev Microbiol* 12, 263-273.
27. Visscher PM, Brown MA, McCarthy MI, Yang J (2012) Five years of GWAS discovery. *Am J Hum Genet* 90: 7-24.
28. Balding DJ (2006) A tutorial on statistical methods for population association studies. *Nat Rev Genet* 7: 781-791.
29. Stephens M, Balding DJ (2009) Bayesian statistical methods for genetic association studies. *Nat Rev Genet* 10: 681-690.
30. Perez-Losada M, et al. (2006) Population genetics of microbial pathogens estimated from multilocus sequence typing (MLST) data. *Infect Genet Evol* 6, 97-112.
31. Vos M, Didelot X (2009) A comparison of homologous recombination rates in bacteria and archaea. *IMSE J* 3, 199-208.

32. Price, A. L., Patterson, N. J., Plenge, R. M., Weinblatt, M. E., Shadick, N. a., & Reich, D. (2006). Principal components analysis corrects for stratification in genome-wide association studies. *Nature Genetics*, *38*(8), 904–9. doi:10.1038/ng1847
33. Besier, S., Ludwig, A., Brade, V., & Wichelhaus, T, A., (2003) Molecular analysis of fusidic acid resistance in *Staphylococcus aureus*. *Molecular Microbiology*, *47*(2), 463-469.
34. O’Neill, A. J., & Chopra, I. (2006) Molecular basis of fusB-mediated resistance to fusidic acid in *Staphylococcus aureus*. *Molecular Microbiology*, *59*(2), 664-676.
35. O’Neill, a J., McLaws, F., Kahlmeter, G., Henriksen, a S., & Chopra, I. (2007) Genetic basis of resistance to fusidic acid in staphylococci. *Antimicrobial Agents and Chemotherapy*, *51*(5), 1737-1740.
36. Neil, A. J. O., Larsen, A. R., Henriksen, A. S., & Chopra, I. (2004). A Fusidic Acid-Resistant Epidemic Strain of *Staphylococcus aureus* Carries the fusB Determinant, whereas fusA Mutations Are Prevalent in Other Resistant Isolates, *48*(9), 3594-3597.
37. Lippert C, et al. (2011) FaST linear mixed models for genome-wide association studies. *Nat Methods* 8: 833-835.
38. Zhou X, Stephens M (2012) Genome-wide efficient mixed-model analysis for association studies. *Nat Genet* 44: 821-824.
39. Yang, J., Zaitlen, N., Goddard, M., (2014) Advantages and pitfalls in the application of mixed-model association methods. *Nature*. *46*(2), 100-106.
40. Listgarten, J., et al., (2012) Improved linear mixed models for genome-wide association studies. *Nature methods*. *9*(6) 525-526.
41. Felsenstein, J. (1985) Phylogenies and the comparative method. *Am Nat* 125: 1-15.
42. Grafen, A. (1989) The phylogenetic regression. *Phil Trans Roy Soc B* 326: 119-157.
43. Milkman R, Bridges MM (1990) Molecular evolution of the *Escherichia coli* chromosome. III. Clonal frames. *Genetics* 126: 505-517.
44. Hedge, J., Wilson, D. J. Bacterial phylogenetic reconstruction from whole genomes is robust to recombination but demographic inference is not. *mBio* 5: e02158-14 (2014).
45. Didelot, X., Wilson, D.J. ClonalFrameML: efficient inference of recombination in whole bacterial genomes. *PLoS Comput Biol* 11, e1004041 (2015).
46. McVean, G. (2009) A genealogical interpretation of principal components analysis. *PLoS Genet* 5: e1000686.
47. Hoffman, G. E. Correcting for population structure and kinship using the linear mixed model: theory and extensions. *PLoS ONE* 8: e75707 (2013).
48. Wald, A. (1943). Tests of statistical hypotheses concerning several parameters when the number of observations is large. *Trans. Amer. Math. Soc.*, *54*(3), 426-482.
49. Walker, T.M., et al. Whole genome sequencing for prediction of *Mycobacterium tuberculosis* drug susceptibility and resistance: a retrospective cohort study. *Lancet Infect. Dis.* 15, 1193-1202 (2015).
50. Gordon, N.C., et al. Prediction of *Staphylococcus aureus* antimicrobial resistance by whole-genome sequencing. *J. Clin. Microbiol.* 52, 1182-1191 (2014).
51. Stoesser, N., et al. Predicting antimicrobial susceptibilities for *Escherichia coli* and *Klebsiella pneumoniae* isolates using whole genome sequence data. *J. Antimicrob. Chemother.* 68, 2234-2244 (2013).
52. Pupko, T., Pe’er, I., Shamir, R., & Graur, D. A fast algorithm for joint reconstruction of ancestral amino acid sequences. *Mol. Biol. Evol.* 17, 890-896 (2000).
53. Browning, S.R. & Browning, B.L. Rapid and accurate haplotype phasing and missing data inference for whole genome association studies by use of localized haplotype clustering. *Am. J. Hum. Genet.* 81,1084-97 (2007).
54. Bradley, P., et al. (2015) Rapid antibiotic resistance predictions from genome sequence data for *S. aureus* and *M tuberculosis*. Biorxiv <http://dx.doi.org/10.1101/018564>

55. O'Hagan, A., & Forster, J. (2010) *Kendall's Advanced Theory of Statistics Volume 2B Bayesian Inference*, Second Edition. Chapter 11, The Linear Model. Wiley-Blackwell, Oxford.
56. Eyre, D. W. *et al.* (2012) A pilot study of rapid benchtop sequencing of *Staphylococcus aureus* and *Clostridium difficile* for outbreak detection and surveillance. *BMJ Open* 2:e001124
57. Everitt, R. G. *et al.* (2014) Mobile elements drive recombination hotspots in the core genome of *Staphylococcus aureus*. *Nat. Commun.* 5, 3956.
58. Lunter, G. & Goodson, M. (2011) Stampy: a statistical algorithm for sensitive and fast mapping of Illumina sequence reads. *Genome Res.* 21:936-939.
59. Zerbino, D. R. & Birney, E. (2008) Velvet: algorithms for de novo short read assembly using de Bruijn graphs. *Genome Res.* 18:821-829.
60. Hyatt D, Chen GL, Locascio PF, Land ML, Larimer FW, Hauser LJ. (2010) Prodigal: prokaryotic gene recognition and translation initiation site identification. *BMC Bioinformatics.* 8,11(1):119.
61. Weizhong Li & Adam Godzik. (2006) Cd-hit: a fast program for clustering and comparing large sets of protein or nucleotide sequences. *Bioinformatics* 22,1658-1659
62. Rizk, G., Lavenier, D., & Chikhi, R. (2013). DSK: k-mer counting with very low memory usage. *Bioinformatics*, 29(5), 652-653.
63. Bolger, A.M., Lohse, M., & Usadel, B. (2014) Trimmomatic: a flexible trimmer for Illumina sequence data. *Bioinformatics* 30, 2114-2120.
64. Stamatakis, A. (2014) RAxML version 8: a tool for phylogenetic analysis and post-analysis of large phylogenies. *Bioinformatics*, 30(9), 1312-3
65. Pupko, T., Pe'er, I., Shamir, R., Graur, D., (2000) A fast algorithm for joint reconstruction of ancestral amino acid sequences. *Molecular biology and evolution.* 17(6), 890-896.
66. Yahara, K., Didelot, X., Ansari, M., Sheppard, S. K., & Falush, D. (2014) Efficient Inference of Recombination Hot Regions in Bacterial Genomes. *Molecular Biology and Evolution* 31(6):1593-1605.
67. Dunn, O. J. (1959). Estimation of the medians for dependent variables. *The Annals of Mathematical Statistics*, 192-197.
68. Camacho, C. *et al.* (2009) BLAST+: architecture and applications. *BMC Bioinformatics* 10:431.
69. Langmead, B., Salzberg, S. (2012) Fast gapped-read alignment with Bowtie 2. *Nature Methods.* 9:357-359.
70. UniProt Consortium. (2015) UniProt: a hub for protein information. *Nucleic Acids Res.* 43:D204-12.

## Acknowledgements

We would like to thank Jean-Baptiste Veyrieras, Deborah Charlesworth and Brian Charlesworth for comments on the manuscript, Xiang Zhou and Matthew Stephens for helping adapt their software and Xavier Didelot, Daniel Falush, Rory Bowden, Zam Iqbal, Chris Spencer, Simon Myers, Jonathan Marchini, Joe Pickrell, Peter Visscher, Alkes Price and Peter Donnelly for useful discussions. This study was supported by the Oxford NIHR Biomedical Research Centre and the UKCRC Modernising Medical Microbiology Consortium, the latter funded under the UKCRC Translational Infection Research Initiative supported by the Medical Research Council, the Biotechnology and Biological Sciences Research Council and the National Institute for Health Research on behalf of the UK Department of Health (Grant G0800778) and the Wellcome Trust (Grant 087646/Z/08/Z). D.W.C. is an NIHR Senior Investigator. D.J.W. is a Sir Henry Dale Fellow, jointly funded by the Wellcome Trust and the Royal Society (Grant 101237/Z/13/Z).

### **Author contributions**

S.G.E, C.-H.W., J.C., D.J.W. designed the study, developed the methods, performed the analysis, interpreted the results, wrote the manuscript. D.A.C. commented on the manuscript. N.S., N.C.G., T.M.W., E.G.S., N.I., M.J.L., T.E.P., D.W.C., A.S.W. designed and implemented isolate collection and whole-genome sequencing and assisted interpretation. G.M., A.S.W. assisted methods development and writing the manuscript.

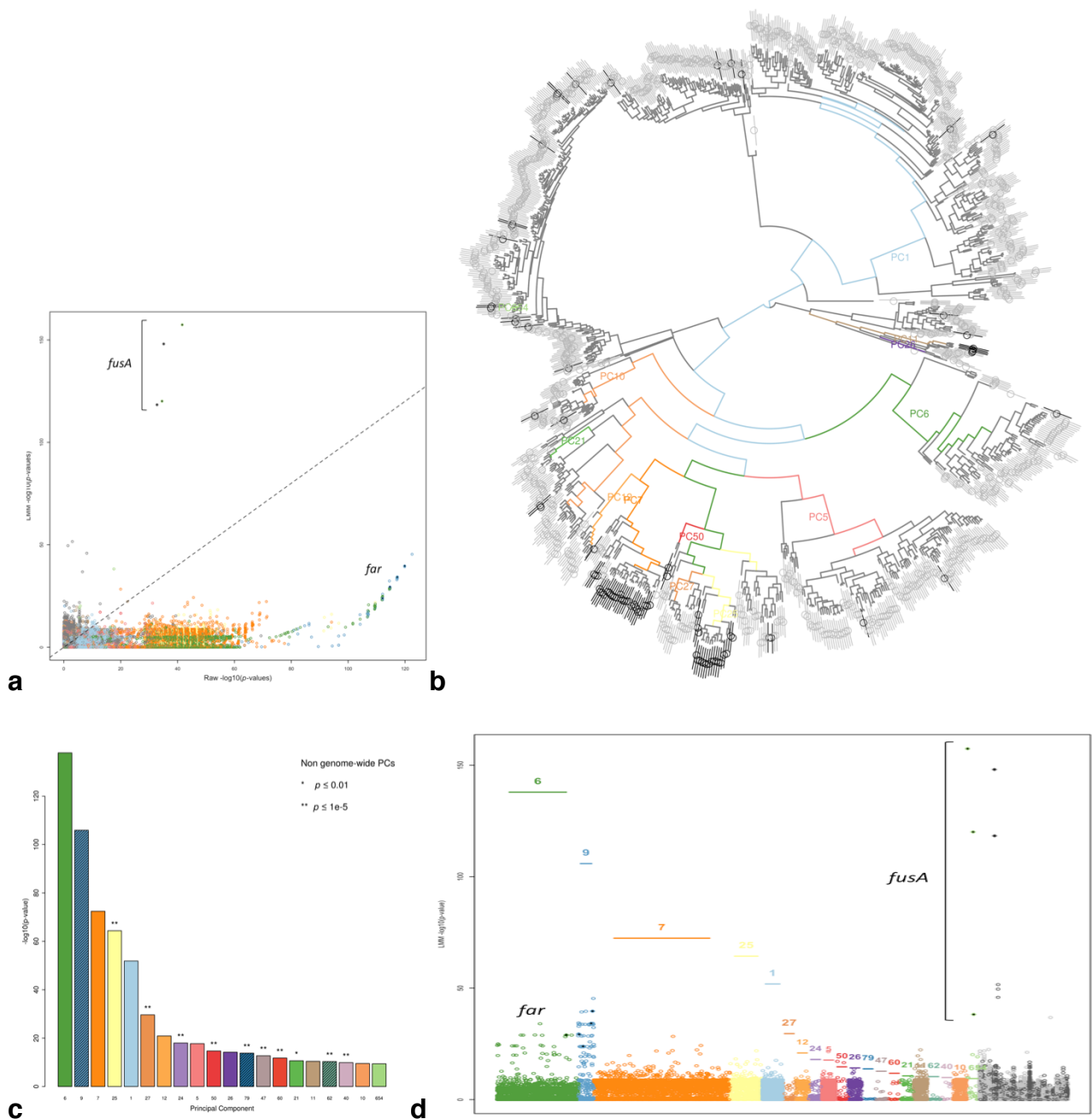


**Figure 1.** Controlling for population structure in bacterial GWAS for fusidic acid resistance in *S. aureus*. **(a)** Effect of controlling for population structure using LMM on significance of the presence or absence of 31bp kmers. Only 400,000 kmers are plotted: the 200,000 most-significant kmers prior to control for population structure and a random 200,000. Each kmer is colour-coded according to the PC to which it is most strongly correlated, grey if it is not most strongly correlated to one of the 20 most significant PCs by the Wald test. *far* and *fusA* are plotted as diamonds filled with black. **(b)** PCs correspond to dominant lineages in the clonal genealogy. Branches are colour-coded according to the PC to which they are most strongly correlated. Individual genomes are colour-coded with black or grey lines to indicate fusidic acid resistance and susceptibility respectively. The circle passing through the line is colour-coded to indicate the predicted phenotype based on the LMM. Asterisks beside the bars, e.g. PC 25, indicate evidence for lineages associated with particular genomic regions. **(c)** Wald tests of significance of lineage-specific associations. Some PCs, e.g. PC 9, are hashed to indicate that no branch in the clonal genealogy was most strongly correlated with it. Asterisks again indicate non-genome-wide PCs and their *p*-values. **(d)** Manhattan plot showing significance ( $-\log_{10}$  *p*-values) after controlling for population structure, with variants clustered by PC. The horizontal ordering is randomised, and *far* and *fusA* are plotted as diamonds filled with black. This allows identification of the variants corresponding to the most significant lineage-specific associations.

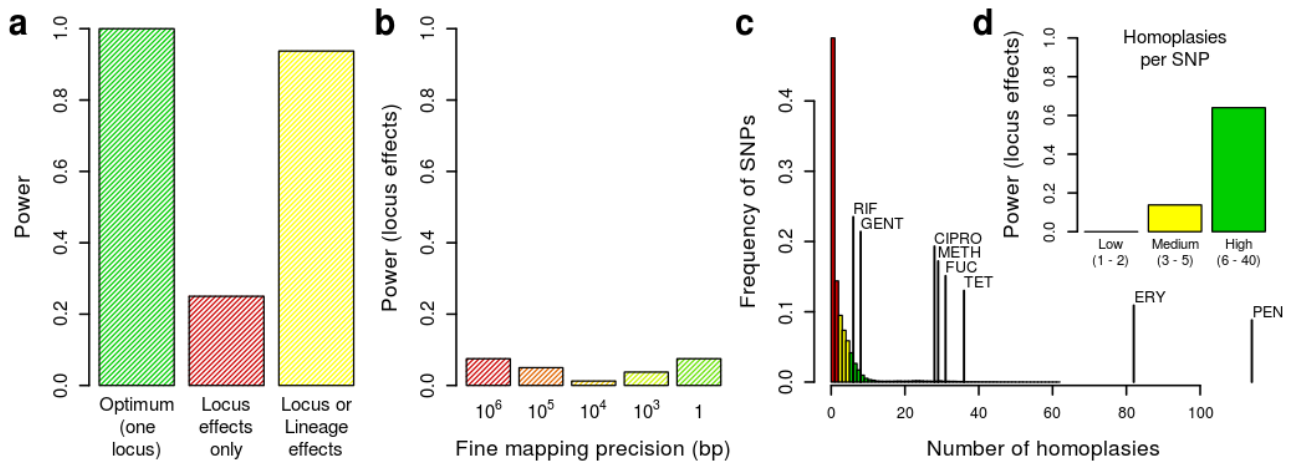
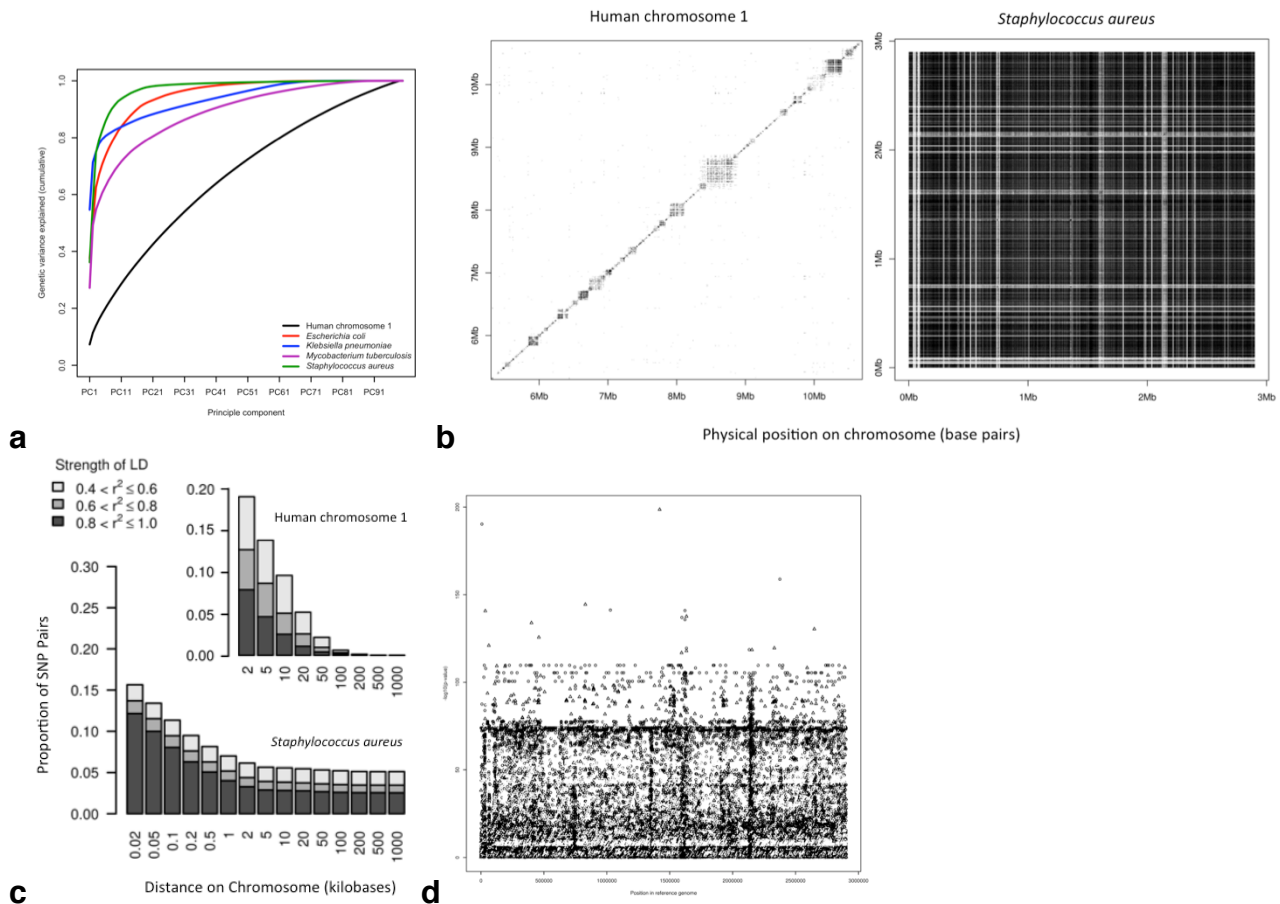


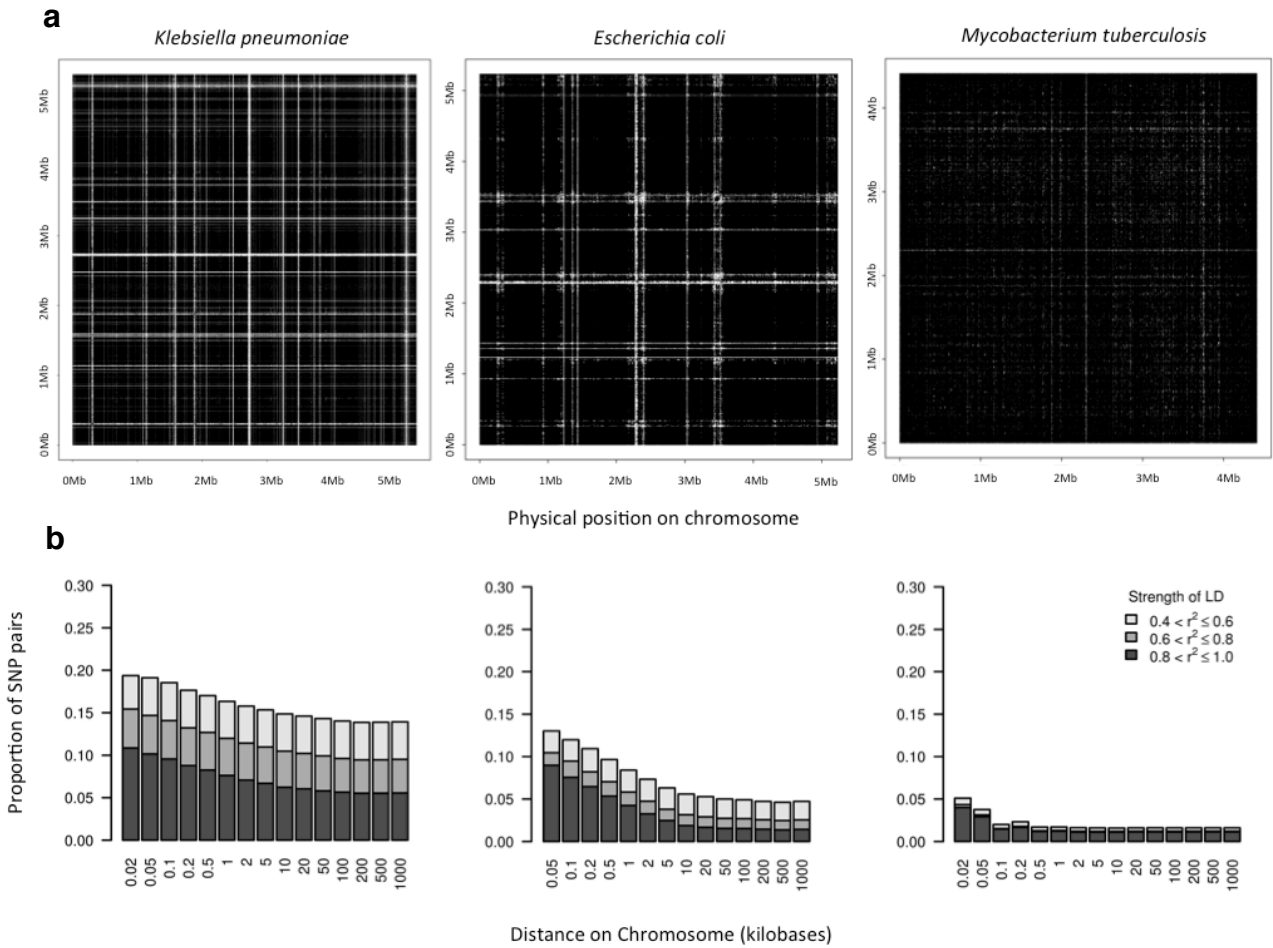
**Figure 2.** Power, fine mapping and homoplasy in *S. aureus*. Simulation results. **a)** Controlling for population structure and multiple testing lead to a drastic reduction in power to detect locus effects, compared to the theoretical optimum power for a single locus. The Wald test improves power several-fold by detecting lineage-specific effects. **b)** Fine mapping precision is very coarse in bacteria owing to genome-wide LD. Interpreting lineage effects can be helpful when the locus-specific signal cannot be fine-mapped. **c)** The number of times common SNPs (MAF>20%) and antibiotic resistance phenotypes have emerged on the phylogeny. **d)** When homoplasy is high, power to detect locus effects is much improved, explaining the good power to map antibiotic resistance phenotypes. In the simulations, causal loci were selected at random from high frequency SNPs (MAF>20%) in the  $n = 992$  isolates, with case probabilities of 0.25 and 0.5 for the common and rare alleles respectively (odds ratio of 3). Genome wide significance (to detect locus effects) was based on a Bonferroni-corrected  $p$ -value threshold of  $\alpha$ , equal to 0.05 divided by the number of SNP patterns.





**Supplementary Figure 1.** Population structure and linkage disequilibrium in humans vs *S. aureus*. The structure of linkage disequilibrium (LD) in bacteria is strikingly different to humans. **(a)** The leading principal components explain a much greater proportion of genetic variability in the bacterial species than in human chromosome 1, indicating that a greater proportion of variants are population stratified. **(b)** Points show sites in LD ( $r^2 > 0.7$ ). In contrast to the block-like structure of LD in humans, in *S. aureus* the genome comprises one large LD block because of strong population structure and limited homologous recombination. **(c)** LD decays rapidly in bacteria, as in humans, but plateaus to residual levels resulting in genome-wide LD. **(d)** Manhattan plot showing the significance of the association ( $-\log_{10} p$ -value) between each SNP and ciprofloxacin resistance in *S. aureus*, before controlling for population structure. The horizontal bands are signatures of genome-wide LD.





**Supplementary Figure 2.** Population structure and linkage disequilibrium in *K. pneumoniae*, *E. coli*, *M. tuberculosis*. (a) Points show sites in LD ( $r^2 > 0.7$ ). (b) LD decays rapidly in bacteria, as in humans, but plateaus to residual levels resulting in genome-wide LD.

ATGGATATAGTTTCTTTATGGGACAAAACCCTACAATTAATAAAAAGGTGACT

- ATGGATATAGTTTCTTTATGGGACAAAACCC (1) *Trim adaptors*  
TGGATATAGTTTCTTTATGGGACAAAACCCT (2) *Remove duplicates*  
GGATATAGTTTCTTTATGGGACAAAACCCTA (3) *Remove low quality reads*  
GATATAGTTTCTTTATGGGACAAAACCCTAC (4) *Count 31 base kmers (DSK)*  
ATATAGTTTCTTTATGGGACAAAACCCTACA (5) *Deduplicate kmers*  
TATAGTTTCTTTATGGGACAAAACCCTACAA (6) *Annotate kmers by BLAST*  
ATAGTTTCTTTATGGGACAAAACCCTACAAT (7) *Test each for association*  
TAGTTTCTTTATGGGACAAAACCCTACAATT  
AGTTTCTTTATGGGACAAAACCCTACAATTA

**a**

(1) *Assemble reads with Velvet*



(2) *Annotate open reading frames on contigs (Prodigal)*

MDDAYYGLFYEDVKHV\* MLFTALSNLNSNAILPVRLDGV\*

(3) *Cluster proteins into groups of  $\geq 70\%$  similarity with Cd-hit*

MTAGFLLNMSSIIDKKIYVLSKNNMVEKTSSK\* \* <- cluster represented by longest sequence  
MTAGFLLNMSSIIDKKIYVLSKNNMVEK\*  
MTAGFLLNMSSIIDKKIYVLSKNNMVEK\*  
MTAGFLLNMSSIIDKKIYVLSKNNMVEKTSSK\*

(4) *BLAST against contigs to assess presence/absence of each gene*

>GENE1 0 1 1 1 1 1  
>GENE2 0 0 0 0 0 1  
>GENE3 1 0 1 0 0 1

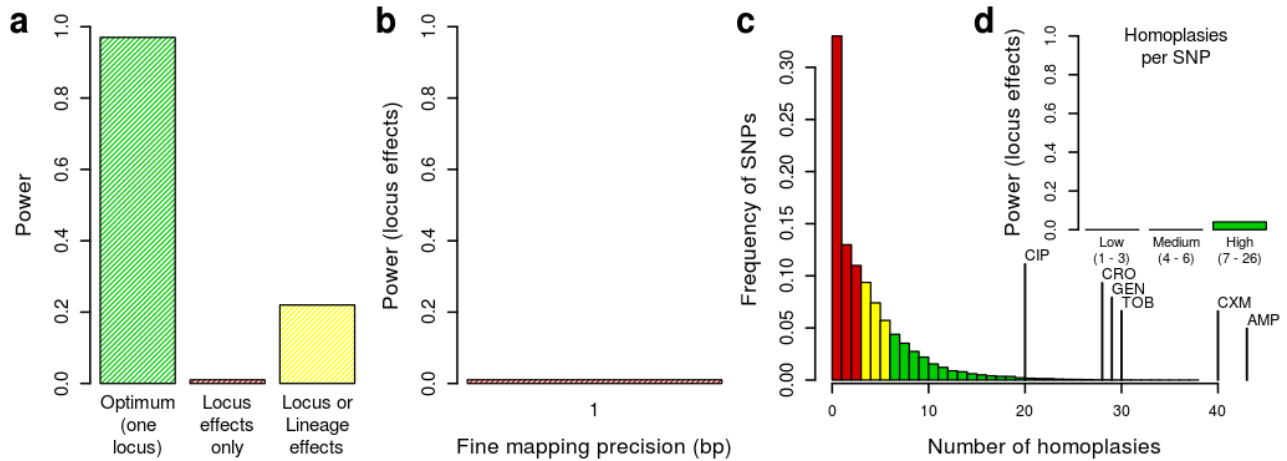
(5) *Test each gene for association with phenotype*



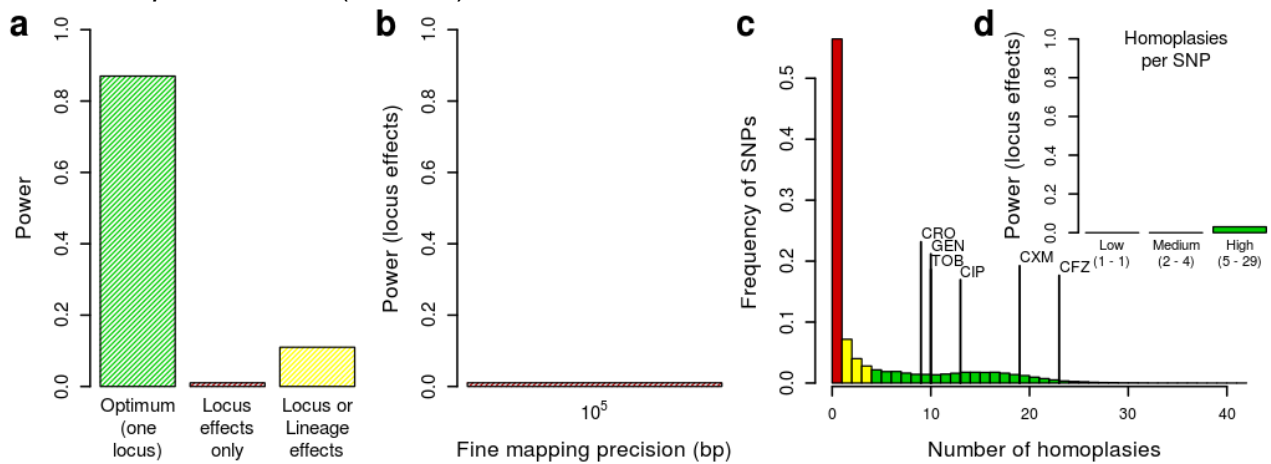
**b**

**Supplementary Figure 3.** (a) Kmer analysis of hard-to-reach diversity. Some diversity (e.g. indels, repeats) is difficult to capture using standard variant calling tools. We directly analyse presence/absence of short haplotypes (*kmers*) to make sure we don't miss any associations. (b) Capturing the accessory genome. Differential presence or absence of genes or entire mobile elements is an important source of diversity in bacterial genomes. We test for associations with gene presence/absence by defining the accessory genome and profiling each bug.

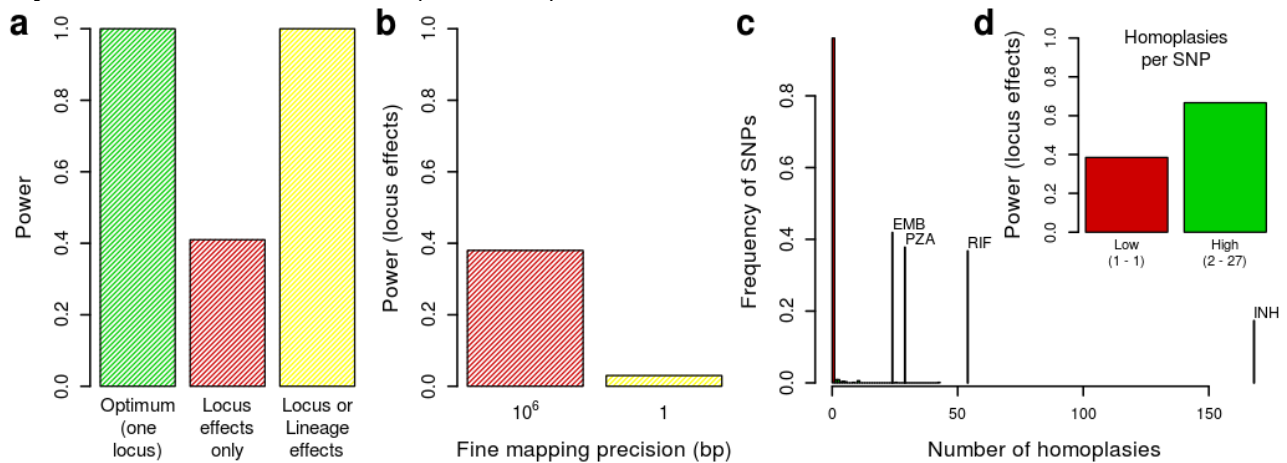
*Escherichia coli* (n = 241)



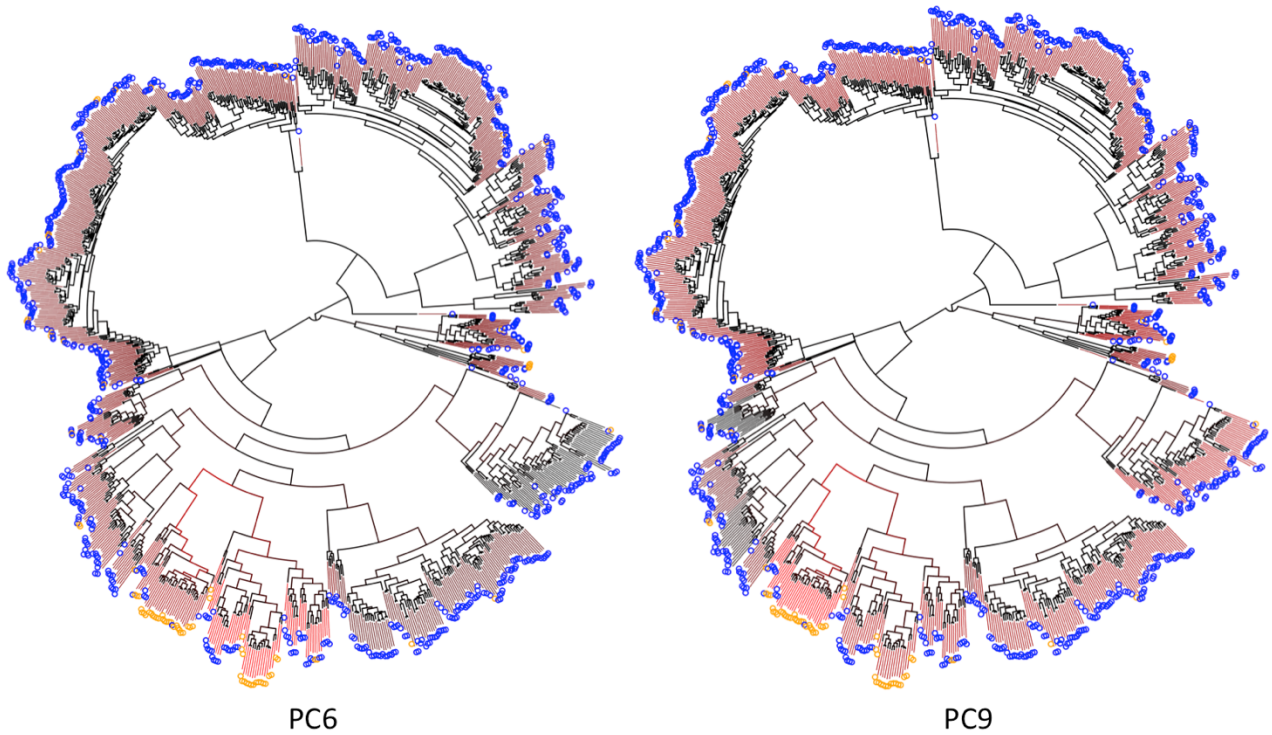
*Klebsiella pneumoniae* (n = 176)



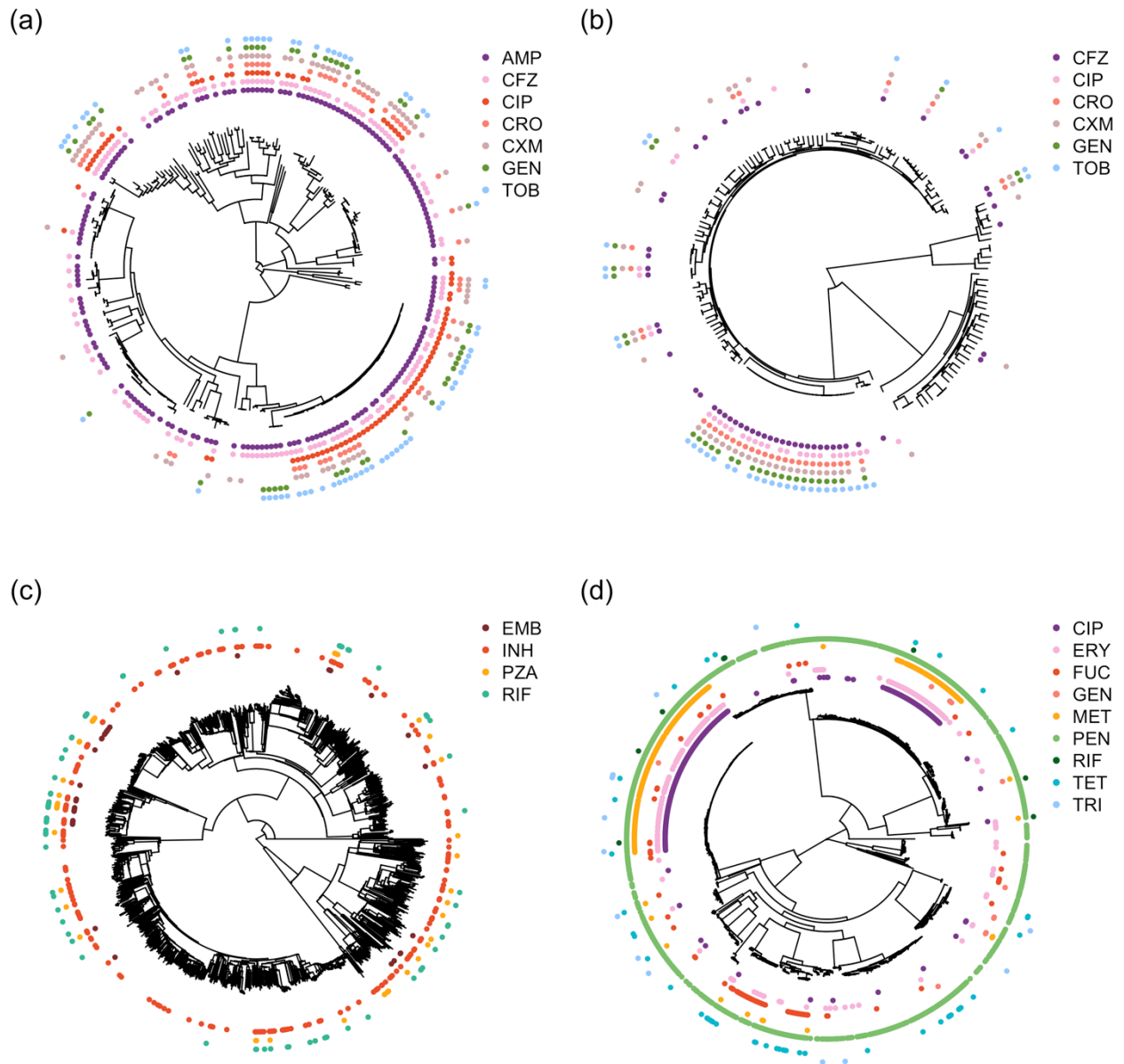
*Mycobacterium tuberculosis* (n = 1954)



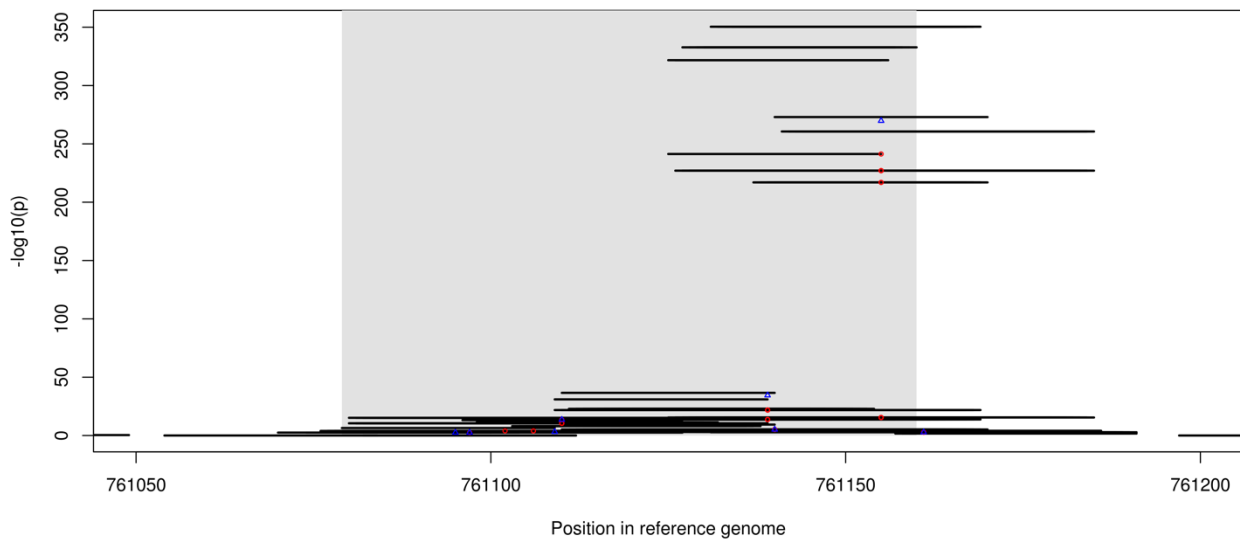
**Supplementary Figure 4.** Power, fine mapping and homoplasies in *E. coli* (top row), *K.pneumoniae* (middle row) and *M. tuberculosis* (bottom row). Simulation results. **a**) Controlling for population structure and multiple testing lead to a drastic reduction in power to detect locus effects, compared to the theoretical optimum power for a single locus. The Wald test improves power several-fold by detecting lineage-specific effects. **b**) Fine mapping precision is very coarse in bacteria owing to genome-wide LD. Interpreting lineage effects can be helpful when the locus-specific signal cannot be fine-mapped. **c**) The number of times common SNPs (MAF>20%) and antibiotic resistance phenotypes have emerged on the phylogeny. **d**) When homoplasies is high, power to detect locus effects is much improved, explaining the good power to map antibiotic resistance phenotypes. In the simulations, causal loci were selected at random from high frequency SNPs (MAF>20%) in the *n* isolates, with case probabilities of 0.25 and 0.5 for the common and rare alleles respectively (odds ratio of 3). Genome wide significance (to detect locus effects) was based on a Bonferroni-corrected *p*-value threshold of  $\alpha$ , equal to 0.05 divided by the number of SNP patterns.



**Supplementary Figure 5.** The *S. aureus* phylogeny with branches coloured by correlation with Principal Components (PCs) 6 and 9, and tips annotated by fusidic acid resistance (orange circles) or sensitivity (blue circles). Branches are coloured according to their strength of association with the PC, from black (not correlated) to red (strongly correlated). Tips of the phylogeny are annotated with coloured lines according to the projections of the individual onto the PC, rescaled between 0 and 1 (from black to red).



**Supplementary Figure 6.** Evolutionary relationships and distribution of antibiotic resistance in the four species: (a) *Escherichia coli* (n = 241), (b) *Klebsiella pneumoniae* (n = 176), (c) *Mycobacterium tuberculosis* (n = < 1954) and (d) *Staphylococcus aureus* (n = ≤992). In each case the midpoint-rooted maximum likelihood clonal frame tree is shown. AMP = Ampicillin, CFZ = Cefazolin, CIP = Ciprofloxacin, CRO = Cefuroxime, CXM = Ceftriaxone, GEN = Gentamicin, TOB = Tobramycin, EMB = Ethambutol, INH = Isoniazid, PZA = Pyrazinamide, RIF = Rifampicin, ERY = Erythromycin, FUC = Fusidic acid, GEN = Gentamicin, MET = Methicillin, PEN = Penicillin, RIF = Rifampicin, TET = Tetracycline, TRI = Trimethoprim.



**Supplementary Figure 7.** A close up of the *rpoB* gene from the *M. tuberculosis* rifampicin GWAS results after controlling for population structure. The grey bar represents the codon positions within *rpoB* where an amino acid change results in resistance. Kmers were plotted as black lines, with their significance of association with rifampicin resistance after controlling for population structure on the y-axis. Blue triangles are all non-synonymous, nonsense and read-through SNP GWAS results after controlling for population structure. The kmers were annotated with the SNPs they contain, with red circles representing all SNPs within the grey bar that were either non-synonymous, nonsense or read-through. The most significant SNP was a non-synonymous SNP causal of resistance, and the most significant kmer also covered this region. However, the kmer was more significant, due to an increase in power by pooling over multiple variants. This is shown by the ‘wild-type’ kmer containing no SNPs, thus it was found to be protective.

Antibiotic	# R	# S	Resistance mechanism	SNP / gene rank	SNP / gene LMM rank	Kmer rank	Kmer LMM rank
<i>E. coli</i>							
Ampicillin	189	52	β-lactamase genes <i>blaTEM</i>	1	1	6 (tnp)	6 (tnp)
Cefazolin	62	179	β-lactamase genes <i>blaCTX-M</i>	2 ( <i>nmpC</i> )	3 ( <i>nmpC</i> )	121710 ( <i>nmpC</i> )	3690 ( <i>nmpC</i> )
Cefuroxime	81	160	β-lactamase genes <i>blaCTX-M</i>	1	1	1598 (162-192 upstream <i>blaCMY-2</i> )	470 (162-192 upstream <i>blaCMY-2</i> )
Ceftriaxone	55	186	β-lactamase genes <i>blaCTX-M</i>	1	1	1403 (tnp)	470 (tnp)
Ciprofloxacin	91	150	SNPs in <i>gyrA<sup>a</sup></i> , <i>gyrB</i> , <i>parC<sup>b</sup></i> or <i>parE</i> or presence of PMQR	1 <sup>b</sup>	1 <sup>b</sup>	1 <sup>b</sup>	1 <sup>a</sup>
Gentamicin	48	193	AAC ( <i>aac(3)-II</i> ), ANT, APH or rRNA methylase	1	1	1	1
Tobramycin	67	174	AAC ( <i>aac(3)-II</i> ), ANT, APH or rRNA methylase	1	1	1	1
<i>K. pneumoniae</i>							
Cefazolin	38	138	β-lactamase genes <i>blaCTX-M</i>	1 + HP + WbuC	1	762 (tnp)	837 (tnp)
Cefuroxime	46	130	β-lactamase genes <i>blaCTX-M</i>	1 + HP + WbuC	1 + HP + WbuC	762 (tnp)	1480 (tnp)
Ceftriaxone	35	141	β-lactamase genes <i>blaCTX-M</i>	1 + HP + WbuC	1 + HP + WbuC	771 (tnp)	812 (tnp)
Ciprofloxacin	34	142	SNPs in <i>gyrA</i> , <i>gyrB</i> , <i>parC</i> or <i>parE</i> or presence of PMQR ( <i>qnr-B1<sup>a</sup></i> , <i>qnr-B19<sup>b</sup></i> )	2 <sup>a</sup> (tnp)	2 <sup>a</sup> (tnp)	1853 <sup>b</sup> (tnp)	4427 <sup>b</sup> (tnp)
Gentamicin	31	145	AAC ( <i>acc(3)-II</i> ), ANT, APH or rRNA methylase	1	1	1	79 ( <i>tmrB_2</i> )
Tobramycin	36	140	AAC ( <i>acc(3)-II</i> ), ANT, APH or rRNA methylase	1	1	1	1
<i>M. tuberculosis</i>							
Ethambutol	41	1589	<i>embB</i>	2 ( <i>rpoB</i> )	1	1	1
Isoniazid	239	1470	<i>katG</i> , <i>mabA</i> or <i>fabG1</i>	1	1	1	1
Pyrazinamide	45	1662	<i>pncA</i>	142 ( <i>rpoB</i> )	1	126 ( <i>rpoB</i> )	1
Rifampin	86	1487	<i>rpoB</i>	1	1	1	1
<i>S. aureus</i>							
Ciprofloxacin	242	750	<i>grlA</i> or <i>gyrA</i>	1	1	1	1
Erythromycin	216	776	<i>ermA</i> , <i>ermC</i> , <i>ermT</i> or <i>msrA</i>	1	1	1	1
Fusidic acid	84	908	SNPs in <i>fusA<sup>a</sup></i> or presence of <i>fusB</i> or <i>far<sup>b</sup></i>	4 <sup>b</sup> ( <i>SAS0037</i> )	1 <sup>a</sup>	75 <sup>b</sup> ( <i>SAS0040</i> )	1 <sup>a</sup>
Gentamicin	11	981	<i>aacA/aphD</i>	1 + GNAT acetyltransferase	1 + GNAT acetyltransferase	1 + 415 bases upstream to 100 bases downstream	1 + 415 bases upstream to 100 bases downstream
Penicillin	824	168	<i>blaZ</i>	1	1	2 ( <i>bla</i> )	2 ( <i>bla</i> )
Methicillin	216	776	<i>mecA</i>	1	1 + <i>mecR1</i>	1 + SCC <i>mec</i> genes	1 + SCC <i>mec</i> genes
Tetracycline	46	946	<i>tetK</i> , <i>tetL</i> or <i>tetM</i>	2 ( <i>repC</i> )	2 ( <i>repC</i> )	1 + plasmid genes	1 + plasmid genes
Trimethoprim	15	308	SNPs in <i>dfrB</i> , presence of <i>dfrG</i> or <i>dfrA</i>	1	1	1	1
Rifampicin	8	984	<i>rpoB</i>	1	1	1	1

**Table 1** Number of resistant and sensitive isolates by species and antibiotics, known mechanisms of resistance and main results. The rank of the most significant result for an expected causal mechanism for each GWAS is reported, plus in brackets the gene that was most significant when it was not causal. Where more than one gene or mechanism causes resistance, the variant we found was underlined, or referred to by <sup>a</sup> and <sup>b</sup>. R = Resistant. S = Sensitive. HP = Hypothetical Protein, tnp = transposase. See Supplementary tables 3-6 for more detail.

Resistance determined by gene presence

Resistance determined by SNPs

Resistance determined by gene presence or SNPs or both

Most significant variant was the expected mechanism

Most significant variant was in physical linkage (PL) with the expected Mechanism

Most significant variant was not the expected mechanism or in PL with the expected mechanism



Species	GWAS studies	Reference genome for mapping	# Bialelic SNPs	# Triallelic SNPs	# Tetra-allelic SNPs	# Kmers	# Gene clusters
<i>Staphylococcus aureus</i>	Ciprofloxacin, Erythromycin, Fusidic acid, Gentamicin, Penicillin, Methicillin, Tetracycline, Rifampicin	<i>Staphylococcus aureus</i> MRSA252 (GenBank accession no. BX571856.1)	264604	14731	519	24154606	13881
	Trimethoprim	<i>Staphylococcus aureus</i> MRSA252 (GenBank accession no. BX571856.1)	196996	8712	269	15840354	10261
<i>Escherichia coli</i>	$\beta$ -lactam: Ampicillin, Ceftazidime, Cefuroxime, Ceftriaxone; Quinolone: Ciprofloxacin; Aminoglycoside: Gentamicin, Tobramycin	<i>Escherichia coli</i> CFT073 (Genbank accession AE014075.1)	430185	25298	1287	39918870	23502
<i>Klebsiella pneumoniae</i>	$\beta$ -lactam: Ampicillin, Ceftazidime, Cefuroxime, Ceftriaxone; Quinolone: Ciprofloxacin; Aminoglycoside: Gentamicin, Tobramycin	<i>Klebsiella pneumoniae</i> subsp. <i>pneumoniae</i> MGH 78578 (GenBank accession no. CP000647.1)	654425	63639	5029	53816250	21382
<i>Mycobacterium tuberculosis</i>	Ethambutol	<i>Mycobacterium tuberculosis</i> H37Rv (GenBank accession no. NC_000962.2)	107481	954	8	15680376	-
	Isoniazid	<i>Mycobacterium tuberculosis</i> H37Rv (GenBank accession no. NC_000962.2)	110401	1020	10	15941713	-
	Pyrazidamide	<i>Mycobacterium tuberculosis</i> H37Rv (GenBank accession no. NC_000962.2)	110163	1012	10	15963479	-
	Rifampin	<i>Mycobacterium tuberculosis</i> H37Rv (GenBank accession no. NC_000962.2)	101969	864	8	15554437	-

Supplementary Table 1. Variant information for all GWAS studies.



Species	% Ns to impute at the site	Sites originally imputed by CFML		Sites originally called		Allele frequency at the site	Sites originally imputed by CFML		Sites originally called	
		% Correct imputation CFML	% Correct imputation Beagle	% Correct imputation CFML	% Correct imputation Beagle		% Correct imputation CFML	% Correct imputation Beagle	% Correct imputation CFML	% Correct imputation Beagle
<i>Escherichia coli</i>										
	0-10%	97.6	98.0	96.5	97.6	0.00-0.01	92.0	89.3	93.2	91.9
	10-20%	96.0	96.5	94.9	95.6	0.01-0.05	90.6	86.9	90.9	88.1
	20-30%	94.8	95.1	94.0	94.3	0.05-0.10	91.4	90.5	91.8	90.5
	30-40%	94.6	94.7	93.7	93.9	0.10-0.15	92.6	92.4	91.9	91.6
	40-50%	92.3	91.1	91.9	90.9	0.15-0.20	93.8	93.5	92.9	92.8
	50-60%	93.4	92.8	93.0	92.1	0.20-0.25	93.0	93.3	91.9	92.1
	60-70%	92.3	89.6	91.7	89.0	0.25-0.30	93.8	94.5	92.3	93.1
	70-80%	91.0	89.0	90.1	87.7	0.30-0.35	94.9	95.0	93.3	93.4
	80-90%	88.2	83.5	87.1	82.8	0.35-0.40	96.4	96.3	94.6	94.8
	90-100%	82.9	74.3	81.7	73.4	0.40-0.45	98.0	97.9	96.5	96.9
						0.45-0.50	97.3	97.7	96.1	97.0
<i>Klebsiella pneumoniae</i>										
	0-10%	95.8	93.7	95.8	94.3	0.00-0.01	90.1	86.5	92.1	88.6
	10-20%	92.9	91.2	92.0	90.1	0.01-0.05	90.9	88.5	92.3	89.8
	20-30%	90.4	88.4	91.3	89.2	0.05-0.10	91.8	91.2	92.3	91.2
	30-40%	94.8	94.1	95.6	94.6	0.10-0.15	93.7	93.5	94.9	94.3
	40-50%	94.6	94.4	95.8	95.1	0.15-0.20	93.1	92.5	94.3	92.9
	50-60%	95.6	95.3	96.6	96.0	0.20-0.25	91.7	91.1	96.0	94.5
	60-70%	94.6	93.8	95.6	94.3	0.25-0.30	84.6	85.8	84.5	87.2
	70-80%	92.8	90.7	94.0	90.6	0.30-0.35	85.0	85.0	82.1	85.7
	80-90%	80.7	78.1	79.7	76.1	0.35-0.40	85.4	85.2	82.2	85.9
	90-100%	82.5	72.7	83.9	71.6	0.40-0.45	90.2	90.5	86.0	89.3
						0.45-0.50	94.2	93.2	88.4	91.7
<i>Mycobacterium tuberculosis</i>										
	0-10%	99.8	98.0	99.8	99.0	0.00-0.01	93.8	86.4	96.8	94.9
	10-20%	99.9	98.7	99.8	99.0	0.01-0.05	98.4	81.9	98.3	90.2
	20-30%	99.7	98.7	99.8	98.8	0.05-0.10	99.5	91.8	99.8	93.8
	30-40%	99.5	97.8	99.7	98.3	0.10-0.15	98.4	88.3	99.6	94.3
	40-50%	99.9	98.4	99.7	98.4	0.15-0.20	100	97.1	100.0	96.7
	50-60%	99.4	93.6	99.6	98.4	0.20-0.25	100	96.9	99.7	96.2
	60-70%	95.7	94.2	99.0	96.2	0.25-0.30	99.6	93.5	99.9	96.3
	70-80%	98.8	92.3	98.4	95.3	0.30-0.35	100	95.9	100	96.4
	80-90%	98.4	88.4	97.8	91.5	0.35-0.40	100	97.2	100.0	96.0
	90-100%	89.5	72.0	88.3	78.1	0.40-0.45	100	75	100	98.5
						0.45-0.50	NA	NA	NA	NA
<i>Staphylococcus aureus</i>										
	0-10%	98.1	97.7	98.0	97.9	0.00-0.01	84.3	79.8	92.5	89.8
	10-20%	97.0	96.5	97.7	97.1	0.01-0.05	87.5	80.7	91.4	85.9
	20-30%	93.9	92.8	94.9	94.4	0.05-0.10	88.4	80.8	92.7	88.8
	30-40%	89.2	85.2	91.7	88.2	0.10-0.15	90.2	86.4	91.5	87.8
	40-50%	91.7	87.2	93.7	89.6	0.15-0.20	91.8	90.1	92.9	90.5
	50-60%	87.5	79.0	90.7	84.4	0.20-0.25	91.0	89.1	92.9	90.8
	60-70%	85.9	77.5	89.0	82.3	0.25-0.30	93.9	91.0	94.3	91.4
	70-80%	88.7	81.2	91.1	84.6	0.30-0.35	95.7	93.5	95.3	93.6
	80-90%	85.6	79.3	88.4	82.9	0.35-0.40	95.9	95.9	95.2	95.4
	90-100%	73.8	67.4	77.5	69.1	0.40-0.45	96.7	96.8	95.9	96.2
						0.45-0.50	97.3	96.8	95.0	96.4

Supplementary Table 2 Imputation accuracy for ClonalFrameML and Beagle per species. Results have been stratified into accuracy for sites which were originally imputed using ClonalFrameML, and accuracy for sites which were originally all called, so that the results are not biased by the original imputation by ClonalFrameML.

Antimicrobial agent	Gene	Study	Variant	Genome position (in reference genome) or BLAST accession		Alleles	Type	Ctrl 1	Ctrl 2	Ctrl 3	Case 1	Case 2	Case 3	Odds ratio	-log10(p)	Rank	-log10(p) LMM	Rank LMM
				Pre-LMM	LMM													
CIP	<b>griA</b>	SNP / gene	S80F, S80Y, F80Y	1419998		C, T, A	NS, NS, NS	745	5	0	14	226	2	2405.3, Inf, Inf	198.6	1	138.2	1
		Kmer		1419968-1420098				745	5	-	18	224	-	1854.2	190.5	1	99.1	9
		Kmer		1419995-1420025				22	728	-	228	14	-	0.002	177.2	46	113.6	1
	<b>gyrA</b>	SNP / gene	S84L	7255		C, T	NS	745	5	-	20	222	-	1653.9	190.3	2	81.6	2
		Kmer		7726 - 7756				6	744	-	223	19	-	0.0007	188.3	23	82.3	47
	ERY	<b>ermC</b>	SNP / gene	Q2FDD1					774	2	-	103	113	-	424.6	85.0	1	193.5
Kmer				NC_022228.1 (743-781)	NC_022228.1 (279-309)			770	6	-	102	114	-	143.4	94.7	1	192.4	12
<b>ermA</b>		SNP / gene	P0A0H3					775	1	-	121	95	-	608.5	70.7	12	75.7	3
<b>ermT</b>		SNP / gene																
<b>msrA</b>		SNP / gene	P0A086					3	773	-	0	216	-	Inf	0.6	1526 46	0.04	203745
		Intergenic, 30bp upstream to <i>ermC</i>	Kmer		AE002098.2 (75634-75664)			772	4	-	106	110	-	200.3	93.1	92	195.7	1
FUS	<b>fusA</b>	SNP / gene	L461-, L461S, -461S	601084		T, A, C	Nonsense, NS, read-through	908	0	-	83	1	-	Inf	11.0	9754	62.3	1
		kmer		601054-601084				1	907	-	18	66	-	0.004	41.6	1158 76	157.4	1
	<b>far</b>	SNP / gene	Q8GNY5					908	0	-	40	44	-	Inf	54.3	4	19.3	39
		kmer		NC_002953.3 (53216-53246)				908	0	-	36	48	-	Inf	119.9	75	39.7	58
	<b>fusB</b>	SNP / gene	Q8GNY5					908	0	-	76	8	-	Inf	9.6	1849 4	16.6	76
	<i>SAS0040</i>	Kmer					908	0	-	35	49	-	Inf	122.5	1	45.4	36	
	<i>SAS0037</i>	SNP / gene					908	0	-	38	46	-	Inf	57.0	1	28.5	21	
	<i>SAS0040</i>	SNP / gene					908	0	-	38	46	-	Inf	57.0	1	28.5	21	



GEN	<b><i>aacA/aphD</i></b>	SNP / gene	P0A0C1				981	0	-	2	9	-	Inf	21.1	1	380.8	1
		Kmer	-	AY971367.1 (727-2683)				981	0	-	2	9	-	Inf	177.4	1	380.8
	<b><i>GNAT acetyltransferase</i></b>	SNP / gene	D2J631				981	0	-	2	9	-	Inf	21.1	1	380.8	1
MET	<b><i>mecA</i></b>	SNP / gene	P60185				773	4	-	3	212	-	13656.3	209.6	1	374.9	1
		Kmer		NC_022604.1 (78438- 78468)				772	4	-	3	213	-	13703	208.2	1	375.6
	HP in SCC-mec	SNP/gene					773	4	-	3	212	-	13656.3	209.6	1	374.9	1
PEN	<b><i>blaZ</i></b>	SNP / gene	P00807				145	23	-	28	796	-	179.2	118.6	1	140.1	1
		Kmer		NC_022604.1 (2824752-2824782)				143	25	-	9	815	-	518.0	166.4	2	210.5
	<b><i>blaI</i></b>		NC_022604.1 (2822414-2822444)				142	26	-	7	817	-	637.4	167.8	1	216.2	1
RIF	<b><i>rpoB</i></b>	SNP / gene	H481Y	592271	C, T	NS	983	1	-	3	5	-	1638.3	11.1	1	158.6	1
		kmer		592260-592290				2	982	-	6	2	-	0.0007	122.0	1	177.9
TET	<b><i>tetK</i></b>	SNP / gene	B0FYM6				945	1	-	9	37	-	3885	58.0	2	315.4	2
		Kmer		KM281803.1 (1198-1228)				945	1	-	4	42	-	9922.5	192.6	1	464.1
	<b><i>tetL</i></b>																
	<b><i>tetM</i></b>																
	<b><i>repC</i></b>	SNP / gene	Q5701				944	2	-	6	40	-	3146.7	62.9	1	364.6	1
TRI	<b><i>dfrB</i></b>	SNP / gene	F99Y	1497290	A, T	NS	308	0	-	10	5	-	Inf	7.9	1	28.5	1
		Kmer		1497269- 1497299				308	0	-	10	5	-	Inf	23.8	1	28.5
	<b><i>dfrG</i></b>	SNP/gene					308	0	-	12	3		Inf	4.9	2	16.1	1
	<b><i>dfrA</i></b>																
	<b><i>orfU1</i></b>	SNP/gene					308	0	-	12	3		Inf	4.9	2	16.1	1
<b><i>LPXTG surface protein</i></b>	SNP/gene					301	7	-	9	6		28.7	5.6	1	13.5	2	

cluster with *tetK* in the pan-genome

clusters with *dfrG* in pan-genome

**Supplementary Table 3. *Staphylococcus aureus* results. CIP = Ciprofloxacin, ERY = Erythromycin, FUS = Fusidic acid, GEN = Gentamicin, MET = Methicillin, PEN = Penicillin, RIF = Rifampicin, TET = Tetracycline, TRI = Trimethoprim. Case = phenotypically resistant, control = phenotypically sensitive. Gene names are coloured according to their resistance causing mechanism, red if it's presence determines resistance, blue if substitutions within the gene causes resistance. Causal genes are in bold.**

Antimicrobial agent	Gene	Study	Variant	Genome position (in reference genome) or BLAST accession		Alleles	Type	Ctrl 1	Ctrl 2	Ctrl 3	Case 1	Case 2	Case 3	Odds ratio	-log <sub>10</sub> (p)	Rank	-log <sub>10</sub> (p) LMM	Rank LMM	
				Pre-LMM	LMM														
AMP	<b>β-lactamase genes</b>	SNP / gene	<i>blaTEM-208</i>	<a href="#">NC_017659.1</a>				51	1	-	59	130	-	112.4	20.1	1	19.4	1	
		Kmer	<i>blaTEM-208</i>	NC_017654.1 (1455 - 1485)				52	0	-	53	136	-	Inf	23.6	6	19.7	6	
		Kmer	Linked to <i>blaOXA-181</i>	KP400525.1 (51445-51475)				50	2	-	43	146	-	84.9	25.9	1	21.2	1	
CIP	<b>gyrA</b>	SNP / gene	D87N, D87W	2626015		C, T, A	NS	147	2	1	5	86	0	1264.2, 0, 0	55.7	2	18.5	2	
		Kmer	-	2626026 - 2626056		-	-	136	14	-	1	90	-	874.3	41.5	45	43.4	1	
	<b>gyrB</b>	SNP / gene		4380590		A, C, G	S	107	35	8	7	39	45	17.0, 86.0, 5.0	26.0	43	21.4	8	
		Kmer																	
	<b>parC</b>	SNP / gene	S80I	3595065		G, A	NS	136	14	-	1	90	-	874.3	59.6	1	55.8	1	
		Kmer		3595065 - 3595095				4	146	-	86	5		0.00159	45.6	1	38.7	28	
	<b>parE</b>	SNP / gene	I529L	3610603		T, G	NS	142	8	-	46	45	-	17.4	15.2	6626	14.8	156	
		Kmer		NC_013361.1 (627842 - 627812)															
	CFZ	<b>β-lactamase genes</b>	SNP / gene	<i>blaCTX-M-15</i>	U5SQ39				102	0	-	96	43	-	Inf	12.7	2	6	3
			Kmer	<i>blaCTX-M-15</i>	DQ335219.1 (405 - 435)				102	0	-	107	32	-	Inf	6.71	121710	3.99	3690
<i>nmpC</i>		SNP / gene		P21420				15	87	-	91	48	-	0.09	15.4	1	12.4	1	
		Kmer	<i>nmpC</i>	1985557 – 1985587				16	86	-	91	48	-	0.1	13.8	1	9.6	1	

CXM	<b><math>\beta</math>-lactamase genes</b>	SNP / gene	<i>bla</i> CTX-M-14	U5SQ39	159	1	-	39	42	-	171.2	23.2	1	18.99	1
		Kmer	<i>bla</i> CTX-M-15	KP268826.1 (7 - 37)	160	0	-	50	31	-	Inf	16.3	1598	15.4	470
	<i>Intergenic</i>	Kmer	Linked to <i>bla</i> CMY-2 (31177 - 32322)	LC019731.1 (31015 - 31045)	160	0	-	38	43	-	Inf	25.6	1	20.0	1
CRO	<b><math>\beta</math>-lactamase genes</b>	SNP / gene	<i>bla</i> CTX-M-15	<a href="#">NC_022648.1</a>	185	1	-	13	42	-	597.7	34.5	1	48.2	1
		Kmer	<i>bla</i> CTX-M-15	KP268826.1 (7 - 37)	186	0	-	24	31	-	Inf	27.3	1403	34.9	470
	tnpA – ISECP1	Kmer	Linked to <i>bla</i> CTX-M-132 (8362 - 9237; complement )	KM207012.2 (9298 – 9328)	186	0	-	12	43	-	Inf	39.7	1	56.4	1
GEN	<b>ACC</b>	SNP / gene	<i>acc</i> (3)-II	<a href="#">ESD46483.1</a>	192	1	-	9	39	-	832.0	35.5	1	68.4	1
		Kmer	<i>acc</i> (3)-II	CP008735.1(7913-7943)	CP008735.1(7913-7943)	193	0	-	9	39	-	Inf	41.9	1	74.0
TOB	<b>ACC</b>	SNP / gene	<i>acc</i> (3)-II	<a href="#">ESD46483.1</a>	174	0	-	27	40	-	Inf	28.6	1	30.5	1
		Kmer	<i>acc</i> (3)-II	KJ850481(134-164)	KJ850481(134-164)	174	0	-	27	40	-	Inf	28.2	1	30.5

**Supplementary Table 4. *Escherichia coli* results. AMP = Ampicillin, CEFA = Cefazolin, CEFU = Cefuroxime, CEFT = Ceftriaxone, GEN = Gentamicin, TOB = Tobramycin. Case = phenotypically resistant, control = phenotypically sensitive, ACC = Aminoglycoside N-acetyltransferase genes, ANT = Aminoglycoside N-acetyltransferase genes, APH = Aminoglycoside O-phosphotransferase genes. Gene names are coloured according to their resistance causing mechanism, red if it's presence determines resistance, blue if substitutions within the gene causes resistance. Causal genes are in bold.**

Antimicrobial agent	Gene	Study	Variant	Genome position (in reference genome) or BLAST accession		Alleles	Type	Ctrl 1	Ctrl 2	Ctrl 3	Case 1	Case 2	Case 3	Odds ratio	-log10(p)	Rank	-log10(p) LMM	Rank LMM	
				Pre-LMM	LMM														
				CFZ	<b><i>β-lactamase genes</i></b>														SNP / gene
	Kmer	<i>blaCTX-M-15</i>	DQ335219.1 (110-140)					122	1	-	20	33	-	201.3	20.6	762	15.2	837	
	<i>HP from ISEcp1</i>	SNP / gene						122	1	-	20	33	-	201.3	20.8	1	15.2	2	
	protein WbuC	SNP / gene		AIG86706.1				122	1	-	20	33	-	201.3	20.8	1	15.2	1	
	<i>ISEcp1 tnpA</i>	Kmer	Linked to <i>blaCTX-M-15</i>	EU418923.1 (10812 - 10842, reverse)				122	1	-	19	34	-	218.3	21.3	1	18.3	1	
CXM	<b><i>β-lactamase genes</i></b>	SNP / gene	<i>blaCTX-M-15</i>	A0A075VKM9				129	1	-	13	33	-	327.5	24.2	1	23.4	1	
		Kmer	<i>blaCTX-M-24</i>	NC_022078.1 (127606 - 127633, reverse)				129	1	-	13	33	-	327.5	25.0	772	23.4	1480	
		<i>ISEcp1 tnpA</i>	Kmer	Linked to <i>blaCTX-M-15</i>	EU418923.1 (10812 - 10842, reverse)				129	1	-	12	34	-	365.5	25.9	1	26.6	1
		<i>HP from ISEcp1</i>	SNP / gene						129	1	-	13	33	-	327.5	24.2	1	23.4	1
		protein WbuC	SNP / gene		AIG86706.1				129	1	-	13	33	-	327.5	24.2	1	23.4	1
CRO	<b><i>β-lactamase genes</i></b>	SNP / gene	<i>blaCTX-M-15</i>	<a href="#">AIG86707.1</a>				140	1	-	2	33	-	2310	32.8	1	60.5	1	

		Kmer	<i>bla</i> CTX-M-24	NC_022078.1 (127606 - 127633, reverse)	140	1	-	2	33	-	2310	35.4	762	60.5	803	
	<i>HP from ISEcp1</i>	SNP / gene			140	1	-	2	33	-	2310	32.8	1	60.5	1	
	protein WbuC	SNP / gene		AIG86706.1	140	1	-	2	33	-	2310	32.8	1	60.5	1	
	<i>ISEcp1 tnpA</i>	Kmer	Linked to <i>bla</i> CTX-M-15	EU418923.1 (10812 - 10842, reverse)	140	1	-	1	34	-	4760	36.7	1	76.0	1	
CIP	Plasmid-mediated quinolone resistance genes	SNP / gene	<i>aac(6)-Ib-c</i>	<a href="#">ACV60575.1</a>	138	4	-	8	26	-	112.1	20	5	16.7	4	
		SNP / gene	<i>qnr-B1</i>	<a href="#">A0A075VJL2</a>	140	2	-	9	25	-	194.4	20.7	2	19.5	2	
		SNP / gene	<i>oqxB</i>	V9ZFU7	141	1	-	34	0	-	0	0.29	5756 24	0.2	162054	
		Kmer	<i>qnr-B19</i>	JX298080.1 (481 – 511)	130	2	-	9	25	-	180.6	25.0	1846	19.5	4423	
		tnpA (truncated)	Kmer	Linked to <i>qnr-B19</i>	JX298080.1 (1520 – 1550)	135	7	-	3	31	-	199.3	27.3	1	28.5	1
		tnpA	SNP / gene	Linked to aac	BAD08693.1	131	11	-	2	32	-	190.5	23.5	1	19.9	1
GEN	ACC	SNP / gene	<i>aac(3)-II</i>	<a href="#">AHI38985.1</a>	145	0	-	0	31	-	NA	36.8	1	>100	1	
		Kmer	<i>aac(3)-II</i>	AJD77170.1(383 – 413)	145	0	-	0	31	-	Inf	39.4	1	15.6	397987	
	ANT	SNP / gene	<i>aac(6)</i>	<a href="#">AIG86041.1</a>	141	4	-	5	26	-	183.3	22.1	6	18.6	7	



	APH	SNP / gene	<b><i>aph(3')-1b</i></b>	<a href="#">AHI38995.1</a>	143	2	-	31	0	-	0	0.04	5317 61	0.03	511031
	tmrB_2 (Tunicamycin resistance protein)	Kmer	Linked to aacA4 (314520 – 315119, complement )	CP011314.1 (310752 – 310782)	145	0	-	2	29	-	Inf	36.5	519	146.4	1
TOB	ACC	SNP / gene	<b><i>acc(3)-II</i></b>	AIG86707.1	140	0	-	5	31	-	Inf	30.4	1	43.3	1
		Kmer	<b><i>acc(3)-II</i></b>	LK391770.1 (21132 - 21162)	140	0	-	5	31	-	Inf	33.0	1	43.3	1
	ANT	SNP / gene	<b><i>aac(6)</i></b>	<a href="#">AIG86041.1</a>	139	1	-	7	29	-	575.6	25.6	3	27	3
	APH	SNP / gene	<b><i>aph(3')-1b</i></b>	<a href="#">AHI38995.1</a>	138	2	-	36	0	-	0	0.47	5254 89	0.36	90210

Supplementary Table 5. *Klebsiella pneumoniae* results for drugs where resistance is determined by the presence of a gene. CEFA = Cefazolin, CEFU = Cefuroxime, CEFT = Ceftriaxone, GEN = Gentamicin, TOB = Tobramycin. Case = phenotypically resistant, control = phenotypically sensitive. ACC = Aminoglycoside N-acetyltransferase genes, ANT = Aminoglycoside N-acetyltransferase genes, APH = Aminoglycoside O-phosphotransferase genes. Gene names are coloured according to their resistance causing mechanism, red if it's presence determines resistance, blue if substitutions within the gene causes resistance. Causal genes are in bold.

Antimicrobial agent	Gene	Study	Variant	Genome position (in reference genome) or BLAST accession		Alleles	Type	Ctrl 1	Ctrl 2	Ctrl 3	Case 1	Case 2	Case 3	Odds ratio	- log10(p)	Rank	- log10(p) LMM	Rank LMM
				Pre-LMM	LMM													
				EMB	<i>embB</i>													
Kmer		4247429 - 4247459						31	1558	-	31	10	-	0.006	130.2	1	107.5	1
	<i>rpoB</i>	SNP	S450L, S450W	761155		C, T, G	NS	1563	23	3	17	23	1	91.9, 30.6, 0.333	27.5	1	45.9	2
INH	<i>katG</i>	SNP	S315T	2155168		C, G	NS	1468	2	-	86	153	-	2475.8	151.1	1	169.4	1
Kmer			2155145 - 2155175	2155145 - 2155175				1468	2	-	87	152	-	1282.4	220.9	1	172.4	1
PZA	<i>pncA</i>	SNP	V125G	2288868	2288868	A, C	NS	1662	0	-	41	4	-	Inf	7.2	142	60.0	1
Kmer			2288847 - 2288877	2288847 - 2288877				1662	0	-	41	4	-	Inf	33.3	7890	60.0	1
Kmer								1	1661	-	7	38	-	0.003	50.2	174	25.7	653
	<i>rpoB</i>	SNP	S450L, S450W	761155	761155	C, T, G	NS	1632	28	2	23	21	1	53.2, 35.5, 0.7	22.3	1	54.4	2
RIF	<i>rpoB</i>	SNP	S450L, S450W	761155	761155	C, T, G	NS	1486	0	1	34	49	3	Inf, 131.1, 0	73.2	1	269.8	1
Kmer			761136 - 761166	761136 - 761166				7	1480	-	70	16	-	0.001	250.0	1	0	1
Kmer			761126 - 761156	761126 - 761156				6	1481	-	66	20	-	0.001	237.2	14	321.7	1

Supplementary Table 6. *Mycobacterium tuberculosis* results. EMB = Ethambutol, INH = Isoniazid, PZA = Pyrazinamide, RIF = Rifampicin. Case = phenotypically resistant, control = phenotypically sensitive. Gene names are coloured according to their resistance causing mechanism, red if it's presence determines resistance, blue if substitutions within the gene causes resistance. Causal genes for each antimicrobial agent are in bold.